Petrogenesis and geochemistry of mafic rocks from the Kutná Hora Crystalline Complex and the neighbouring part of the Rataje Micaschist Zone

Jiří K. NOVÁK and Helena VRBOVÁ

Geological Institute, Academy of Sciences of the Czech Republic, Rozvojová 135, 165 02 Praha 6 – Lysolaje, Czech Republic; e-mail: novak@gli.cas.cz

ABSTRACT: Metabasite intercalations related to the major allochtonous units of the Kutná Hora Crystalline Complex [KHCC], the Rataje Micaschist Zone and the para-autochtonous Varied Group of Moldanubicum have been compared in terms of their petrology and major-, trace-, and rare earth element geochemistry. Attention is also focused on the tectonomagmatic affinities of the retrograded eclogite, garnetiferous amphibolite, massive-, striped-, and banded amphibolites as indicators of past plate tectonic setting, and to the igneous protolith. After a brief description of the petrography and mineral chemistry of the main metabasic rock types, some data on geothermobarometry are presented. In places, the amphibolite juxtaposition with a high-pressure retrograded eclogite bodies, predominantly in the uppermost Gföhl Terrane, provides further evidence that complicated tectonometamorphic evolution is indicative of complex uplift tectonics for the KHCC.

KEY WORDS: terrane, retrograded eclogite, amphibolite types, mineral chemistry, geothermobarometry, geochemistry.

1. Introduction

Thirty four samples of metabasic rocks were collected from the *Kutná Hora Crystalline Complex* [KHCC], the *Micaschist Zone* and northern margin of the *Moldanubian Zone* for a petrological-geochemical investigation. All samples were studied petrologically in thin section and chemically by whole-rock and microchemistry analytical techniques. The electron microprobe technique provided access to the mineral chemistry of pyroxene, garnet, amphibole, plagioclase, clinozoisite-epidote, and chlorite. Samples are listed in Appendix 1 and their location is depicted on a simplified geological map (Fig. 1).

This study of the petrology and geochemistry of these metabasic rocks was initiated to (1) determine degree of similarity of the amphibolites to each other in the geological context, (2) distiguish these rocks from the Gföhl Unit and Micaschist Zone, and (3) identify the igneous protolith. Fundamental questions include the one whether these terranes represent a segment of ocean floor obducted onto the continental margin or even whether the terranes contain volcanic and subvolcanic associations formed in an ocean-island setting. The petrological research was conducted within the framework of a grant titled "Development of the selected Variscan terranes in the Bohemian Massif" with J. K. Novák as the principal investigator. RNDr. H. Vrbová participated by solving some of the geochemical problems related to identifying the igneous protolith and by constructing the plots.

2. Geological setting

The Kutná Hora Crystalline Complex [KHCC] of eastern Bohemia, situated between the internal Variscan Moldanubian Zone and the low-grade Proterozoic of the Bohemicum (Mísař et al. 1983), is a fairly complete example of several deep-seated nappes with different lithologies (Matte et al. 1990, Synek and Oliveriová 1993, Medaris et al. 1995). The tectonical and lithostratigraphical analyses of the KHCC by Synek and Oliveriová (1993) have led to the identification of the Běstvina, Malín and Plaňany Formations within the uppermost Gföhl Terrane. The far-travelled Kouřim Nappe and the lowermost Micaschist Zone have their own tectonometamorphic histories. Retrograded eclogite, diablastic- and garnetiferous amphibolites are predominantly widespread within the *Gföhl Unit* and *Moldanubian Zone*, whereas banded or striped amphibolites and massive amphibolite s.s. comprise a part of the *Micaschist Zone*. The *Kouřim Nappe*, which belongs to the Middle Allochthon, consists of gneissified pre-Variscan granites and fine-grained migmatites only, without any metabasic rocks. The area of study lies approximately between the towns of Kutná Hora and Plaňany, and in the neighbouring Micaschist Zone between the towns of Rataje n. S. and Čáslav (Fig. 1).

The high-pressure metabasic rocks of the Běstvina Formation, in the SE part of the study area, are represented by retrograded eclogite and garnetiferous amphibolite, except for the Běstvina omphacite-bearing granulites (Pouba et al., 1987). This formation was terminated by the elongated intrusion of the Svatý Kříž Basic Massif (consisting of coronitic two-pyroxene metagabbro, gabbronorite, anorthositic gabbro, schistose gabbro, and migmatized amphibolites), as described by Munshi (1978, 1981). The massif is located between the villages of Ronov nad Doubravkou and Moravany, about 12 km SE of Čáslav, covering an area of about 4 sq.km (Culek, 1951). An isolated stock of serpentinite lies near Mladotice (Orlov 1930).

The mafic rocks connected to the Malín Formation also belong to differently retrograded eclogite and diablastic- or garnetiferous amphibolites, but massive amphibolites and striped varieties also occur. Some pyroxene amphibolites s.s. from Kbel, Kbílek, Kluky and numerous lenses of the garnetiferous amphibolite, which occurr between Krychlov and Polní Voděrady, near the villages of Mančice, Lošánky, and Kořenice, have been described by Kratochvíl (1947, 1952). The discovery of eclogitic rocks from the serpentinite body in the vicinity of Poličany was reported by Sokol (1925).

The metabasic rocks exposed in the Plaňany Formation were tectonically intercalated with sillimanite-biotite

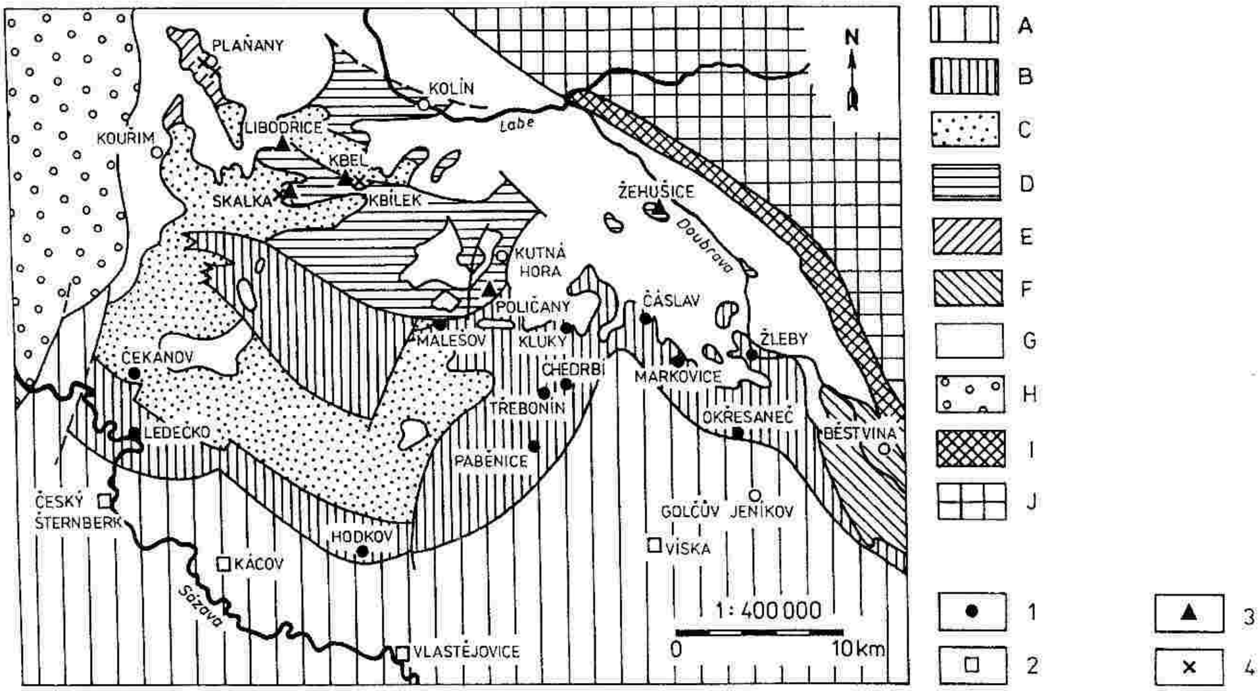

Figure 1. Simplified geological map of the Kutná Hora Crystalline Complex (KHCC), of the Micaschist Zone, and northern part of the Moldanubicum showing sample location
1 – banded amphibolites from the Micaschist Zone
2 – massive amphibolites and garnetiferous amphibolites of the Moldanubicum
3 – retrograded eclogite and diablastic amphibolites from the Malín Formation (uppermost Gföhl terrane)
4 – masive amphibolites and garnetiferous amphibolites of the Plaňany Formation
A – *Moldanubian Zone*: Proterozoic Varied Group
B – *Rataje Micaschist Zone*: metasediments, metabasics, dolostones, calc-silicate rocks, phyllonites
C – *Kouřim Nappe*: gneissified pre-Variscan granite, migmatite
D – *Gföhl Unit-Malín Formation*: blastomylonites, migmatites, metabasics, calc-silicate rocks, orthogneisses
E – *Gföhl Unit-Plaňany Formation*: sillimanite-biotite migmatites, garnetiferous and biotite amphibolites, paragneiss
F – *Gföhl Unit – Běstvina Formation*: granulites (leptynites), orthogneiss with boudins of the retrograded eclogite, garnetiferous amphibolite, and calc-silicate rocks, including the Svatý Kříž Basic Massif
G – *Upper Cretaceous platform sediments*: Cenomanian, Turonian
H – *Permian* sandstones along the Blanice Furrow
I – *Podhořany Crystalline Complex*, hornfelsic paragneiss, mica-schists as relics in two-mica garnet migmatites
J – *Proterozoic of the Železné hory Mts.*: slightly metamorphosed sediments and metaspilites

migmatites and pyroxene-biotite-hornblende migmatites. A paper by Fišera (1981) briefly discusses the varieties of:

(a) abundant amphibolite s.s.
(b) amphibolite with biotite
(c) sphene-biotite and biotite-sphene amphibolite
(d) sporadic garnetiferous amphibolite
(e) sporadic amphibolite with pyroxene admixture
(f) fine-grained melaamphibolite to biotite-hornblende schist
(g) calc-silicate rocks with garnet and plagioclase rimmed by reaction amphibolite. Coarse-grained pyroxenites and serpentinized peridotite are present as rare ultrabasic lenses (up to 65 cm in diameter) with reaction rims lying in the pyroxene-biotite-hornblende migmatites.

The Rataje Micaschist Zone had been previously studied by Koutek (1933, 1939, 1947, 1963, 1965), who interpreted it to be the product of retrogressive metamorphism of Moldanubian rocks and proposed a schematic structural evolution. Sequences of biotite-muscovite micaschist and phyllonite are intercalated with the lenses of banded amphibolites, pyroxene amphibolite s.s., amphibolite to metagabbro and paraamphibolite in connection with some dolostones, marble, calc-silicate rocks and metaquartzite, predominantly along the Sázava river valley and inside the basal rock sequence (Ledečko, Rataje, Malovidy). A more complete petrographical description of the metabasic rocks from this area may be found in Ondřej (1922), Koutek (1933, 1965), and Kratochvíl (1952). A serpentinite body near Kácov has a similar position as the largest serpentinite intrusion near Dolní Kralovice situated on the Sázava-Želivka deep fault zone. Amphibolite-forming metamorphism in the Micaschist Zone is regarded as 478–482 Ma years old, whereas the metamorphism of the Malín Formation occured approximately 499 Ma ago; Rb / Sr method (Gorokhov et al. 1977).

The para-Autochthon comprising the Varied Group of Moldanubian consists of high-grade paragneisses, of migmatized amphibolite lenses showing tholeiitic affinity, and hornblende-biotite gneisses. The pyrope-almandine, high-temperature group A eclogites are widespread in places in the inner part of Moldanubian Zone (Nové Dvory, Biskupice) and of the KHCC (Bečváry) as intercalations in large peridotite bodies (Fediuková 1989, Fiala 1985, Beard et al. 1992, Jakeš et al. 1994). The petrological and geochemical knowledge about retrograded eclogites and diverse amphibolites can shed much light on our understanding of geologic processes that controlled collision-related imbrication (i.e. repeated cycles of transportation).

3. Petrography and geological relations of metabasics

In hand specimens, the analyzed metabasic rocks are structurally variable, either massive-granular (amphibolitic and eclogitic) or banded- and striped amphibolitic in nature. Fracturing on a decimeter scale is associated with veinlets of carbonates and/or epidote. The variability is also due to differing grain sizes and textural phenomena. Modal composition determined from point-counting on all thin sections is given in Appendix 1, Tables 1-3.

Retrograded eclogites

Numerous lenses and float blocks of the common eclogite in paragneiss and migmatite show effects of the retrogressive amphibolite facies metamophism. Their dependence on the size and position of rigid bodies in boudinaged layers is evident. The primary assemblage includes idioblastic garnet (0.5-1 mm) and interstitial diablastic amphibole-plagioclase symplectites II, less often symplectite clinopyroxene. Genetically, during early decompression, the original omphacite became replaced by very fine vermicular symplectites I, formed of diopside and plagioclase. At a more advanced stage of retrogression, the symplectites II, consisting of diablastic amphibole and sodic plagioclase, originated instead of earlier symplectite I.

Disaggregated garnet with a molar proportion of more than 52 % almandine, 32 % grossularite, and 4-7 % pyrope exhibits slight chemical zoning. The pargasitic amphibole in both samples KH-33 and KH-34 (Poličany) encloses some relics of the diablastic amphibole symplectite II. Quartz, ilmenite and rutile inclusions are rare and unevenly distributed. Disequilibrium features comprise coronas of plagioclase around garnet.

In boudins without tectonic movement and extensive metamorphic overprinting, there are equigranular aggregates of pargasitic amphibole, plagioclase and quartz, as well as broken garnet grains. In terms of mineral proportions, the specimens KH-32, KH-34, and KH-21 correspond to the less retrograded eclogites. In addition, the specimens of KH-23, KH-24, KH-25 represent more amphibolized eclogites after dynamic recrystallization. The fracture-related late reactions produced hydrous minerals such as epidote-clinozoisite, and rarely sericite.

The garnetiferous amphibolite (e.g. sample KH-35, Žehušice) displays distinct foliation that is emphasized by the preferred orientation of tschermakitic hornblende. Generally, the skeletal garnet grains are rimmed by medium-grained plagioclase and its alteration products. Sphene, ilmenite, rutile, and rarely apatite and zircon are present as accessory minerals. Retrogressive overprinting is weaker in the isotropic specimens (KH-27, Plaňany Formation), in which garnet grains are slightly pseudomorphed by plagioclase and are now observed as corroded relicts within granoblastic pargasite aggregates. Composition, tectonic layering and association of this variety with retrograded eclogite suggest relationship between both the high-pressure assemblage and amphibolite facies metamorphism. Garnetiferous amphibolite,poor in garnet poikiloblasts (KH-4, Kácov, Moldanubian Zone), include equidimensional grains of Fe-edenitic hornblende and both the coronic plagioclase and quartz pseudomorphs after original garnet. Fractured garnet comprises up to 1.6 % of the mode, whereas the kaolinized plagioclase aggregates, measuring 0.5-1.5 mm across, make up a maximum of 24.5 % of the mode. Occasionally, clinopyroxene, ilmenite, sphene, chlorite, magnetite, and accesory zircon are enclosed within amphiboles. In the quarry of Plaňany, there the tectonically striped varieties of garnetiferous amphibolite display garnet bands of up to 15 mm thickness (Fišera 1981). However, they are volumetrically insignificant. Another type of isotropic and migmatized amphibolite is represented by the sample KH-28 (Vlastějovice) from the Moldanubian Zone. In hand specimen, it is permeated by 2 cm wide pink plagioclase patches caused by beginning migmatization. Under the microscope, the recrystallized early hornblende symplectites with plagioclase (0.1-0.15 mm) without garnet relics are overprinted by concordant ferroedenite. During the retrogressive stage, almost all garnet porphyroblasts were replaced by chloritized biotite pseudomorphs with minor amounts of plagioclase which still preserves its shape. Shear bands consisting of aligned pargasite developed a new foliation. Epidote-clinozoisite, calcite, sphene, ilmenite (leucoxene), quartz, muscovite and goethite may form microinclusions within silicates.

Massive amphibolite s.s.

The isotropic variety of dark amphibolite s.s. shows a gradual transition between sub-ophitic and metamorphically modified nematoblastic texture (KH-31 Víska near Choběbоř, Moldanubian Zone). The primary igneous assemblage is dominated by randomly oriented pargasitic hornblende and interstitial oligoclase with small amounts of quartz and ilmenite. Among accessory minerals, clinozoisite-epidote and clinochlore have been observed.

In a previous paper on amphibolites, Kratochvíl (1952) discussed the petrology of the massive amphibolite with augite and clinozoisite at Kbílek and Mančice (Malín Formation). The same rock-forming assemblage may be found near Český Šternberk and near Poříčko (Koutek 1933, Kaliba 1986). The presence of igneous-looking relics, which preserve the amphibolitized metagabbro, are important in understanding of geologic history of these rocks. They were recognized by Ondřej (1922) and Koutek (1933) in the Micaschist Zone in outcrops near Poříčko.

The banded amphibolite displays diverse alternating dark bands, which are dominant, and subordinate felsic bands. They have a special petrologic significance because of the change from igneous to metamorphic textures and changing metamorphic grade. The mineral assemblage in key samples shows evidence of predominant amphibolite schist (KH-1, Čekanov, KH-2, Ledečko) and strong deformation. The banding is usually shown by variations in mineral composition as well as by differing proportions of the main constituents. The felsic bands, relatively poorer in preferred oriented ferroedenite, are much thinner than the dark ones. Unlike in the dark bands, other minerals are present, e.g. andesine, quartz, sometimes clinozoisite-epidote and calcite in the light bands. Some of the banded amphibolites contain lesser amount of salite and, sometimes, subordinate scapolite. Sphene, apatite, rarely ilmenite, zircon, magnetite, hematite, and chlorite are the dominant accessory phases. The low level of alteration in these rocks is indicated by the small proportion of kaolinite and sericite (after plagioclase). Commonly, banded amphibolites occur as a coherent unit in the micaschists.

Mineralogically, the banded amphibolite shows variation in bulk composition that depends on the composition of the thin separate intercalations. Almost monomineral edenitic schists alternate with:

(1) bands consisting of andesine with a low proportion of Fe-edenite and bands of clinozoisite-epidote (KH-8 and KH-9, Chedrbí, KH-11, Čáslav, KH-12, Žleby, KH-13, Okřesaneč)
(2) bands containing some plagioclase-calcite intergrowths with a lesser amount of clinozoisite-epidote (KH-10, Kluky).

In case (1), the banded amphibolite is interstratified with sillimanite-biotite quartzite and may be similar to the basic metatuffe, as described by Koutek (1963). These rocks usually contain bands with layering concordant with foliation. In a few samples, joint-controlled clinozoisite-epidote and chlorite fillings were found (KH-6). It should be noted that some of the banded amphibolites and, perhaps, some of the paraamphibolites are interbedded with dolostones and calc-silicate rocks (Český Šternberk, Divišov, Malovidy), as pointed out by Kaliba (1986).

Some of the striped amphibolites, in which the granoblastic relics consist of andesine to bytownite, Fe-hornblende or ferroedenitic hornblende, and minor quartz form the second group. The replacement textural relationships show that they are probably recrystallized from fine-grained igneous rock (KH-5 Paběnice, KH-14 Markovice, KH-6 Třebonín). Occasionally, calcite, ilmenite, and clinozoisite-epidote occur as additional phases. Accessory minerals include sphene, apatite, rutile, zircone, and minor amount of chlorite. The grade of metamorphism most likely corresponds to the lower amphibolite facies.

4. Mineral chemistry

In order to evaluate the mineralogical composition and variations at the scale of the individual samples, the representative rock-forming minerals were analyzed in polished thin sections using a JOEL XA-50A type microprobe with EDAX at the Geological Institute of ASCR (analysts M. Kozumplíková and Ing. A. Langrová). An accelering voltage of 15 kV and a sample current of 25 mA were applied; natural standards were utilized. Selected mineral compositions of different metabasic rocks are listed in Appendix 2, Tables 1-7.

Analyses of both the core and margin of grains were performed for each representative mineral from the retrograded eclogite, garnetiferous amphibolite, banded variety of amphibolite, and pyroxene amphibolite. The chemical composition of these rocks is controlled by the relative abundances of pyroxene, amphibole, garnet, plagioclase, clinozoisite-epidote, and chlorite. With regard to their mineral chemistry, the following features are of interest:

Pyroxene

In the least retrograded eclogite (KH-34, Poličany), the symplectite clinopyroxene, present as finely diablastic intergrowth with plagioclase after omphacite, consists of low-Na diopside having a wollastonite component between 45-50 mol.% (Wo = Ca/Ca + Mg + Fe) and of the Al-endiopside (Wo = 23.5 mol. %). The Fs values vary between Fs_{17-18} for endiopside rims and approximately Fs_{16} for Na-diopside core. Due to complete omphacite breakdown, no relics of jadeite-bearing pyroxene have been observed. Occasionally, a very low amounts of $NaAlSi_2O_6$ (Jd) and an appreciable content of Ca (Al, Fe, Ti) Al_{1+x} $Si_{1+x}O_6$ (Ts) as well as low-TiO_2 content are the distinctive features of these pyroxenes. Pyroxenes of the Moldanubian eclogites instead contain diopside-salite up to omphacite (Dudek-Fediuková 1974). In comparison with the Krušné hory eclogite rocks, there is a conspicuous shift in the composition towards the lower content of the jadeite component.

The clinopyroxene composition in the massive amphibolite s.s. (KH-22, Mančice) is slightly different. There, pyroxene grains tend to be Al-diopside with 21–22 mol. % wollastonite (Wo) and 18–19 mol. % hedenbergite (Fs). An appreciable content of Al_2O_3 (Tschermak's component) has also been found. On the other hand, the behaviour of Ca + Mg, Al^{VI} + Na (and Na + Fe^{3+}) confirms the substitution between jadeite and diopside components that is characteristic of an omphacitic trend. According to the new classification of Morimoto (1988), these pyroxenes are augites. Local chemical data on clinopyroxene from the metagabbro (Munshi 1981) indicates the presence of endiopside in the core (42–43 mol. % Wo, 10–11 mol. % Fs) and diopside in the rims (45.6 % Wo, 10 % Fs). Primary low-Ca pyroxene associated with diopside is present only within the two-pyroxene metagabbro from Moravany. The Fs-values of orthopyroxene link enstatite to hyperstene (Fs_{19-20}).

The analyzed clinopyroxene relics enclosed in ferroedenite from specimen KH-8 (Chedrbí) belong to Ca-rich salite having parameters: 200 Wo / (Ca + Mg + Fe)= 104.3 and 100 Fs / (Fs + En)= 34.6. On the diagrams of Leterrier et al. (1982), all clinopyroxenes analyzed fall within the tholeiitic and calc-alkali basalt fields. Available chemical data on pyroxenes are given in Appendix 2, Table 1 together with their structural formulae normalized to six oxygens.

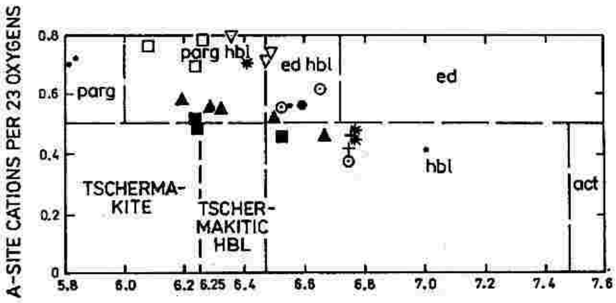

Figure 2. Classification of amphiboles on basis of the $(Na+K)_A$ and the Si (p.f.u.). Symbols as Fig. 3.

Amphibole

Representative analyses of amphiboles from selected metabasic rocks are given in Tables 2a-2d and depicted on Fig. 2. Sodic-calcic amphiboles have been recorded from the retrograded eclogite (Poličany, Libodřice) representing Fe-pargasite to pargasitic hornblende. The number of cations was calculated for amphiboles per 23 oxygen anhydrous formula. The names of amphiboles follow the I.M.A. recommendation based on the Si (p.f.u.) -mg relationship (Leake 1978). The nomenclatorial boundary $(Na + K)_A$= 0.51 atomic units makes the analyzed amphiboles divisible into (a) sodic-calcic (pargasite-) and

(b) calcic (tschermakite) subgroups (over and below 0.50 p.f.u.), both at Ti below 0.50 p.f.u. Secondary magnesio-hornblende is only present within the least retrograded eclogite from Poličany, occurring as a replacement product of pre-existing pargasite. Ferrohornblende has a similar position in the Mančice retrograded eclogite (KH-21).

The calcic amphibole of the migmatized amphibolite from Ronov (Svatý Kříž Basic Massif) is a ferrotschermakitic hornblende (Munshi 1981), when the Si content falls between 6.25 and 6.50 atoms, $(Na + K)_A$ is lower than 0.50, and mg value reaches 0.44.

The amphiboles related to the massive amphibolite may be subdivided into ferroedenite to ferroedenitic hornblende (KH-3, Český Šternberk) and Fe-pargasitic hornblende (KH-31, Víska) on the basis of their structural formulae and mg value. It is interesting that in the banded- and striped amphibolites from Chedrbí and Kbílek (KH-8, KH-19) there is a high content of octahedral Al (Al^{VI} more than 1.00 p.f.u.), and amphibole represents aluminous ferroedenite and aluminous edenite. However, the ferroedenite, edenite, and edenitic hornblende are the common constituents of the majority of these amphibolites. An exception is the banded amphibolite from Markovice (KH-15), where the analyzed amphibole consists of magnesio-hornblende to ferro -hornblende. The composition of amphibole from most of the other banded amphibolites corresponds to pargasitic hornblende in the core and, sometimes, to magnesio-hornblende (KH-17, Malešov) or edenitic hornblende in the rims (KH-29, Hodkov). In garnetiferous amphibolite (KH-35, Žehušice), the growth of tschermakitic hornblende and tschermakite around the pargasitic hornblende relics signals massive recrystallization.

Garnet

Compositional variations of the garnets analyzed differ from grain to grain, and the single grain shows, more or less, some progressive zoning. Some grossularite-almandine with minor pyrope and spessartine molecules (Pyr_{04-07} Alm_{51-55} $Gross_{32-34}$) constitute the retrograded amphibole-bearing MT eclogite (KH-21, Mančice, KH-25, Libodřice). The eclogite-stage garnet (Pyr_{24-50} Alm_{25-50} $Gross_{20-29}$) from Poličany (KH-32, KH-34) is richer in the pyrope molecule than all of the other amphibolized eclogite. This garnet corresponds to that of the transitional- to high-temperature type (HT) group A eclogite occurring in the Moldanubicum (Dudek and Fediuková 1974, Beard et al. 1992). In the diagram by Mottana (1986), the garnet projection points fall into field no. 5 representing layers in ultramafic rocks (Fig. 3). Other garnets from the more retrograded eclogite belong to group C and B eclogite. Rather surprisingly, garnet of the garnetiferous amphibolite from Žehušice (KH-35) falls into field no. 6 of grospydites corresponding to diamondiferous eclogites. The sample of KH-35 emphasizes some conversion of eclogite to garnetiferous amphibolite.

Characteristic features of all these garnets are the depletion of spessartine molecules (0.4 – 1.3 % Spess) and the low – TiO_2 contents. Additional analyses have confirmed that Cr_2O_3 abundance of individual garnet grains is negligible (below 0.12 % Cr_2O_3), but grossularite-almandine (KH-23) is exceptionally richer in Cr_2O_3 (up to 0.61 % Cr_2O_3 on rims).

The second set of data is comprised of garnet analyses of the migmatitized amphibolite of Ronov (Svatý Kříž Basic Massif) and of Plaňany. There, essential grossularite-almandine with slight enrichment of pyrope content (Pyr_{11-12}) on rims has been found by Munshi (1981). However, no distinct compositional zoning in the grains has been established.

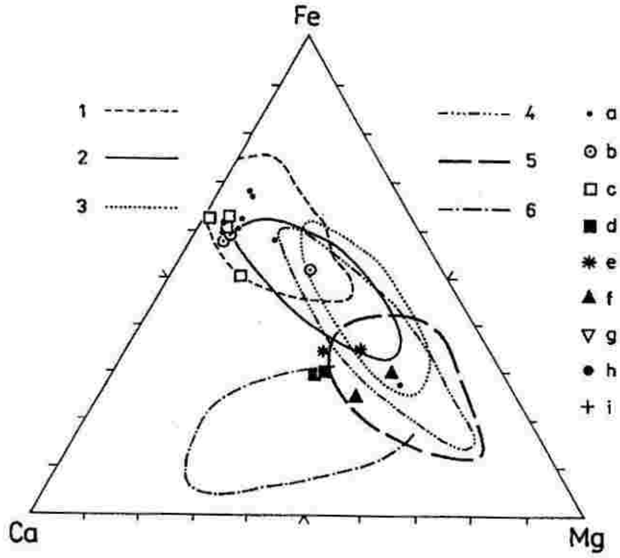

Figure 3. The triangle diagram Ca-Mg-Fe after Mottana (1986), where Ca(= Gross + Andr + Uvar) – Mg (= Pyr) – Fe (= Alm). Fields 1 and 2 refer to group C and B eclogite garnets. Group A garnets are divided in sub-fields: 3 being that of garnet + clinopyroxene + plagioclase-bearing xenoliths in diatremes, also interpreted as granulites: 4 being the field of garnet + clinopyroxene + spinel layers in ultramafic rocks: 5 being that of true eclogites in kimberlite ("griquaites"), and 6: the field of grospydites, diamondiferous eclogites and corundum-bearing eclogites. Points plotted for the samples KH-25, KH-21, KH-23, KH-35, KH-34, and KH-32 are most significant.

It is generally accepted that garnet composition of the garnetiferous amphibolite (Pl-69, Pl-76, Plaňany) is characterized by the predominance of almandine and grossularite and by the variable content of pyrope (Fišera 1981). Table 3 in Appendix 2 gives chemical data on the garnet with its structural formula based on 24 oxygens and end-members in the range Alm-Pyr-Gross-Spess-(Uvar). The negligible amount of ferric iron required on crystallochemical grounds supports the assumption that essentially all of Fe is divalent here.

Plagioclase

Plagioclase in diablastic symplectites of the retrograded eclogite yielded compositions varying from oligoclase to albite (KH-34, Poličany, KH-21,Mančice) and andesine An_{32-36} (KH-32, Poličany).

Plagioclase coronas formed during replacement of garnet in migmatized garnetiferous amphibolite are within the range of andesine (KH-4, Kácov). Some compositional variations of plagioclase from the massive amphibolite represent andesine (KH-3, Český Šternberk) or oligoclase (KH-31, Víska, KH-22, Mančice, "Na skalce").

Plagioclase enclosed in the striped amphibolite (KH-19 Kbílek) grades with continous zoning from bytownite cores (An_{79}) to andesine (An_{36}). The K_2O content is about 0.15 to 1.1 per cent in the core. The albite rims (up to An_{03}) are accompanied by potassium feldspar.

Except for the banded amphibolite of Markovice, andesine is the predominant feldspar in all these rocks.

Plagioclase from Markovice amphibolite (KH-15) shows wide variation in composition from labradorite to andesine. For all analyses, plagioclase formulae were normalized to 32 oxygens (Appendix 2, Tables 4a-4c).

Epidote-clinozoisite group

Confirming results of the petrographic examination, Mn-poor Al-epidote from a striped amphibolite (KH-19 Kbílek) is lower in Fe_2O_3 and is compositionally intermediate between ferrian clinozoisite and epidote. Here, the Al_2Fe-constituent (56.6 – 57.7 mol. %), comprising both the clinozoisite and pistacite molecules, is similar to Al-epidote associated with metamorphic recrystallization of the amphibolite to garnet amphibolite facies (Raith, 1976). The content of the pistacite component (Ps) in Al-epidote from the striped amphibolite varies between Ps_{19-23}, whereas the piemontite component is negligible (0.1 – 0.5 % Pm). According to Liou et al. (1983), the $Fe^{3+}/(Fe^{3+} + Al)$ ratios of epidotes and prehnites vary as a function of oxygen fugacity and temperature. The classification is based on the standard formula of epidote, $Ca_2(Al_{3-x}\ Fe_x)\ Si_3O_{12}(OH)$, where x is below 1.05. Comparison with the skarn Fe-epidote shows an increased content of pistacite molecules (30 % Ps) and 60.5 molar percent of the Al_2Fe component compositionally approaching the stoichiometric pattern. Table 5 gives mineral chemistry recalculated to 12.5 oxygens for anhydrous formulae obtained by electron microprobe analysis and to 13 oxygens for wet analysis of the skarn epidote (sample Z-2, Vlastějovice; Povondra and Žáček, 1991).

Prehnite

Only colourless small crystals were analyzed from a sample of banded amphibolite (KH-19), where prehnite occurs in veinlet filling material. As seen from Table 5 in Appendix 2, a compositionally different variety was reported by Kratochvíl (1934) from the Markovice quarry. The Fe^{3+} content is low, demonstrating metamorphic recrystallization at a temperature much lower than 353 °C, and a pressure less than 5 kbar. Experimental work by Liou et al. (1983) revealed that both the prehnite and epidote became most iron-rich at 325 °C and 2 kb, 353 °C and 5 kbar, or 373 °C and 8 kbar. Chemical composition is characterized by the formula $Ca_2(Al_{1-x}Fe_x)\ (AlSi_3)(OH)_2$ for prehnite, where x is less than 0.5. The anhydrous formula obtained by microprobe analysis was recalculated to 22 oxygens.

Chlorite

The classification recommended by AIPEA Nomenclature Commitee is based on the standard formula $(MgFe^{2+3+}\ Mn,Ni,Cr)_{6-x-y}(Al)_y\ Si_{4-z}Al)\ O_{10}(OH)_8$ (Bailey 1980, Weiss and Ďurovič 1983) and on the assumption that all iron is ferrous. Hey's simple pattern (Hey 1954), based on the relationship between the Si (p.f.u.) and the Fe / (Fe + Mg) ratio in the structural formula, and differing in orthochlorite and leptochlorite (less and more than 4 wt. % Fe_2O_3, respectively), seems to be obsolete (Weiss and Ďurovič 1983). Both the banded and striped amphibolites include single chlorite flakes of the clinochlore-chamosite series. For samples KH-13, KH-29, and KH-6, the Al-Mg-chamosite is most typical. However, in the banded amphibolite from Markovice (KH-15), the Al-Mg-chamosite core and Fe-clinochlore rim has been identified. Chlorite of the striped amphibolite (KH-19, Kbílek) and of the massive amphibolite (KH-31, Víska) falls in the field of Fe-clinochlore.

Some effects of hydrous alteration of the retrograded eclogite must also be considered in regard to the origin of accessory chlorite (Mg-chamosite). Some correlation between the X_{Al} = Al / (Al + Fe + Mg) ratio in chlorites and the metamorphic grade is suggested by Kuniyoshi-Liou (1976). The positive correlation between Al^{IV} and formation temperature in the range of 130-290 °C and linear expression $x = 4.71 \times 10^{-3}$-T8.26 $\times 10^{-2}$ are known from Cathelineau and Nieva (1985). However, the structural formulae must be calculated on the basis of 14 oxygens without Na, K, Ca, and Ti.

Ilmenite

Analyses of the ilmenite slightly altered to leucoxene indicate a relativelly small proportion of pyrophanite component (2.2 – 6 mol. % $MnTiO_3$). The low-Fe_2O_3 ilmenite also contains 0.09 – 4.61 mol. % exsolved hematite lamellae, and oxidition expressed as Fe^{3+} / $(Fe^{3+} + Fe^{2+})$ varies from 0.08 (retrograded eclogite) to 0.09 (banded amphibolite). The structural formulae of ilmenite were recalculated to four cation positions, as shown in Appendix 2, Table 7.

5. Pressure and temperature estimation

Knowledge about pressure-temperature-time paths (P-T-t) from metamorphic rock is needed to distinguish individual histories of lithologic-tectonic units and may be useful for the purpose of this paper. Metamorphic temperatures estimated using the known geothermometers are listed in Appendix 3, Tables 1, 2. Nevertheless, the metamorphic P-T estimations derived here are rather qualitative, because we have dealt with a single observation and a single P-T path, and because the application to natural multicomponent systems remains problematic due to repeated partitioning and re-equilibrations. The P-T paths based on the composition of coexisting ferromagnesian silicates are apparent from Fe-Mg partitioning ($ln\ K_D$), e.g. between the garnet – clinopyroxene (Powell 1985, Ellis and Green 1979) and garnet – hornblende pairs (Graham and Powell 1984) or the amphibole-plagioclase assemblage (Blundy and Holand 1990). In those analyses, for which only the total FeO contents are known, the empirical ferric iron corrections for geobarometry and geothermometry determination in metamorphic rocks are necessary (Schumacher 1991). Here, the obtained microprobe analyses of garnet and pyroxene were improved according to criteria by Mottana (1986). The total FeO contents for each analysis of pyroxene were converted into Fe^{3+} and Fe^{2+} using the equation by Ryburn et al. (1976): $Fe^{3+} = 4 - 2Si - 2Ti - Al - Cr + (Na + K)$. For garnet, calculating the charge imbalance as: $8 - 2Si - 2Ti - Al - Cr + Na = Fe^{3+}(+ Mn^{3+})$ has been used. Pressure estimations are based on the geobarometer by Kohn and Spear (1989).

At our present stage of knowledge, the coexistence of symplectic Al-endiopside and sodic plagioclase as well as garnet and pargasite from the least retrograded massive eclogite (KH-32 Poličany), shows equilibrium conditions of about 20.1 kb at 1008 °C, or about 15.3 kb at 602 °C

(Table 1 in Appendix 3). According to Joanny et al. (1991), the width of pyroxene and plagioclase lamellae in two-mineral symplectites is a function of their formation temperature. Application of the garnet-amphibole geothermometer to the correct Fe, Mg, Ca data in retrograded eclogite (KH-34) yields temperatures ranging from about 694 °C at an assummed pressure of 18.5 kb to 580 °C at pressure of 16.9 kb. In a sample of the more retrograded eclogite (KH-21, Mančice), geothermometric estimations showed equilibrium temperatures of about 507 °C at a pressure of 12.6 kb, or about 592 °C at 13.6 kb. The majority of these eclogitic rocks comprise rather medium-temperature varieties according to the classification of Carswell (1990). Only temperatures higher than 900 °C at a minimum pressure of 12 kb seem to be adequate with respect to the transitional pyrope-almandine eclogite from the inner Moldanubian Zone. There, Fediuková (1989) inferred conditions of 900-1200 °C at 25-30 kb for pyrope-almandine eclogites, and Medaris (1985) gave temperatures and pressures in the range of 900-1300 °C and 26-43 kb, respectively, for several Moldanubian garnet peridotites and pyroxenites connected with eclogites, i.e. eclogites indicate equilibration under upper mantle conditions. According to the results of geothermometry for the southwestern part of the Krušné hory Mts., the equilibration of MT eclogites occurred within the range of 550-730 °C at a minimum pressure of 13-15 kb (Klápová 1990). Recently, assemblages with pseudomorphs after coesite were found in the central Krušné hory Mts., indicating a regional ultra-high pressure metamorphism (Schmädicke et al. 1992). The peak metamorphic temperatures range from 840 °C to 910 °C at a pressure of over 29 kb. For more details see Dudek and Fediuková (1974), Fediuková (1989), Klápová (1990), Schmädicke et al. (1992) and Beard et al. (1992).

In the end stage, formation of garnetiferous amphibolites originated isofacially with surrounding metapelites (equilibration under granulite facies). This stage is also recorded by the tschermakitic hornblende growth at the expense of the diablastic symplectites and garnet. Estimated P-T conditions of this amphibolite event are about 606 °C at 13.3 kb (KH-35). They coincide with equilibration typical for MT-eclogite.

It should be noted that textural features, mineral chemistry, and thermobarometric estimations for massive, banded or striped, garnet-free amphibolites are different from high-pressure metabasics. Significantly lower pressures and temperatures representing the upper amphibolite-facies metamorphism are fixed for massive amphibolite from the Moldanubian Zone (KH-3, KH-31). However, massive amphibolites from the Malín Formation may show a stronger metamorphic overprint (KH-22). The empirical method of Plyusnina (1982) based on the total Al content in amphibole and the proportion of anorthite in plagioclase were used to define the pressure and temperature range (Table 2 in Appendix 3). The composition of amphibole included in samples of KH-8, and KH-19 is consistent with a pressures of 7.7 and 8.0 kb at 550 °C and 555 °C, respectively. Banded amphibolites from the Micaschist Zone are estimated to have equilibrated at a minimum pressure of 5.0-6.2 kb and temperature of 530-575 °C. They were formed at the lower amphibolite facies of metamorphism. The retrograde portion of the P-T-t path corresponds to decompression and younger tectonic overprinting. In terms of the pistacite proportion in Al-epidote and of prehnite presence in fractured amphibolite (KH-19, Kbílek), the temperature-pressure range was below 353 °C and 5 kb (transitional lower amphibolite to greenschist facies). A formation temperature of about 265 °C has been calculated for the same specimen according to the chlorite geothermometer (Cathelineau and Nieva 1985). Presence of margarite inclusions in garnet or its pseudomorphs in micaschists at Solopysky (central part of the KHCC) and in the vicinity of Rataje n. S. (Oliveriová 1991) also documents the transitional P-T regime of the lower amphibolite to greenschist facies of metamorphism. Based on the conclusion given above, we believe that the dynamometamorphism was associated with transport and folding during thrusting, and mainly occurred under conditions of epidote-amphibolite facies metamorphism to greenschist facies mylonitization.

6. Geochemistry and palaeotectonic setting

Rock chemistry

Most of the geochemical data in this study, given in Appendix 4, Tables 1-3, is consistent with basalt-related rocks on the basis of the water- and volatile-free silica (44.6-49 % SiO_2) and the TAS diagram (Le Bas et al. 1986, Fig. 4). However, a few analyses fall into the field of tephrites-basanites with 41-44.6 % SiO_2 and is slightly nepheline-normative (KH-8, KH-9, KH-11, KH-13, KH-30). Massive amphibolites from Mančice and Kbílek (KH-22, KH-19), which contain about 12.1 and 11.08 wt. % MgO, respectively, tend to be picrobasalt. Twenty two metabasite samples have a Mg'value [= mol. MgO / (MgO + FeO + 0.9 Fe_2O_3] ranging from 0.2 to 0.7 (Fig. 7), as well as a higher content of both the Ni and Cr, indicating that the MgO-rich metavolcanites have not undergone greater fractionation (e.g. KH-19, KH-20, KH-22). Thus these samples show on the Cr against Ti plot (Pearce 1975) that they possess chemical characteristics reflecting the more primitive ophiolite within the ocean floor basin (OFB) rather than the tholeiitic basalt from the MORB environment. In contrast, boninites from the island-arc tectonic setting, e.g. from the Bonin Islands, Japan, are high-MgO (over 9 wt. %) andesites characterized by high-SiO_2 (over 55 wt. %) and very low-TiO_2 contents (below 0.3 wt. %).

With the exception of five samples, the metabasic rocks in the entire study area show subalkaline characteristics based on the classification of Irvine and Baragar (1971). Tholeiitic affinity is confirmed by the cation ratio plot after Jensen (1976) and by the CaO-MgO-Al_2O_3 diagram (Condie 1982) (Fig. 5a, b). Here, the field of komatiitic tholeiite is only occupied by the massive amphibolite from Mančice (KH-22). Average CIPW normative values (not shown here) sometimes display both olivine and hyperstene, indicating olivine tholeiite composition (KH-4, KH-22, KH-23, KH-24, KH-25, KH-27, KH-30, KH-32).

Following Pearce et al. (1977), these metabasic rocks mainly show characteristics similar to the mid-ocean ridge basalts (field D) or to the ocean-island tholeiites (field E), on the MgO-Al_2O_3-FeO_{tot} discrimination diagram (Fig. 6b). Much controversy may be centred upon the orogenic tectonic setting (field C), within which projection points of the samples KH-5 and KH-9 fall, and upon the continental environment (field A), in which the massive- and banded amphibolites (KH-3, KH-8, KH-12) are plotted, whether the simplified petrogenic discrimination is true or not.

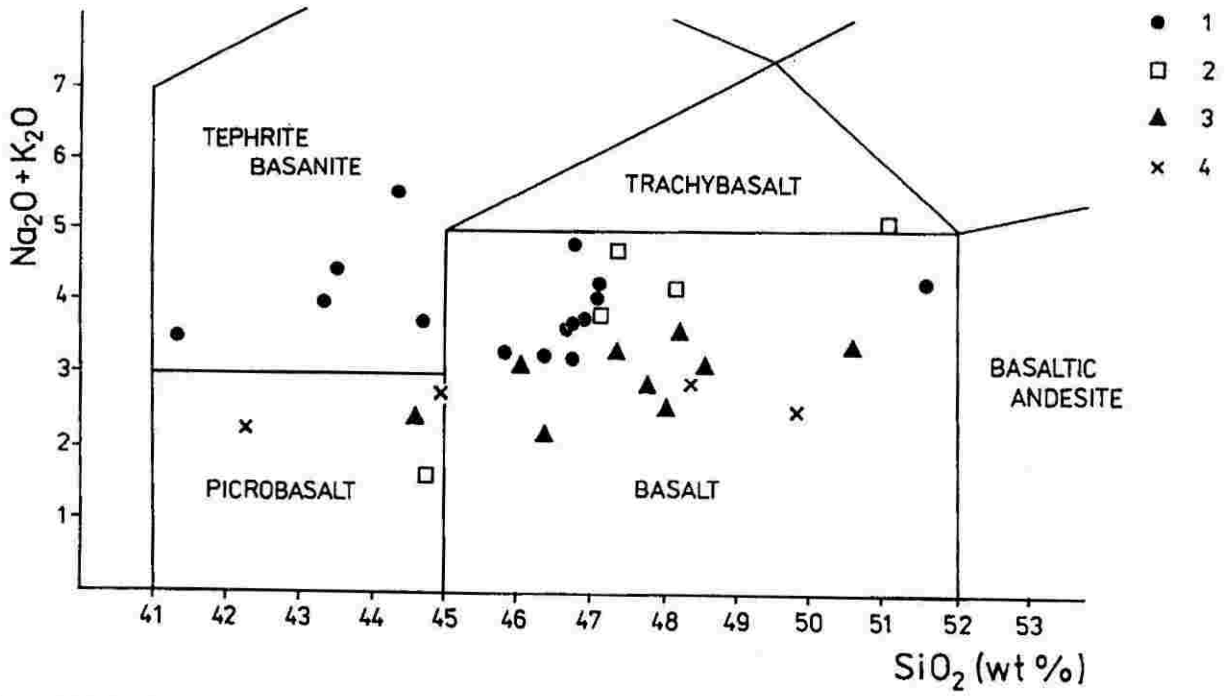

Figure 4. The $Na_2O + K_2O$ versus SiO_2 diagram showing the IUGS classification fields (TAS diagram after Le Bas et al. 1986). Symbols for all the diagrams:
1-banded amphibolites of the Micaschist Zone, 2-metabasics of the Moldanubicum, 3-retrograded amphibolite, 4-diablastic amphibolites 5-garnetiferous amphibolite of the Plaňany Formation.

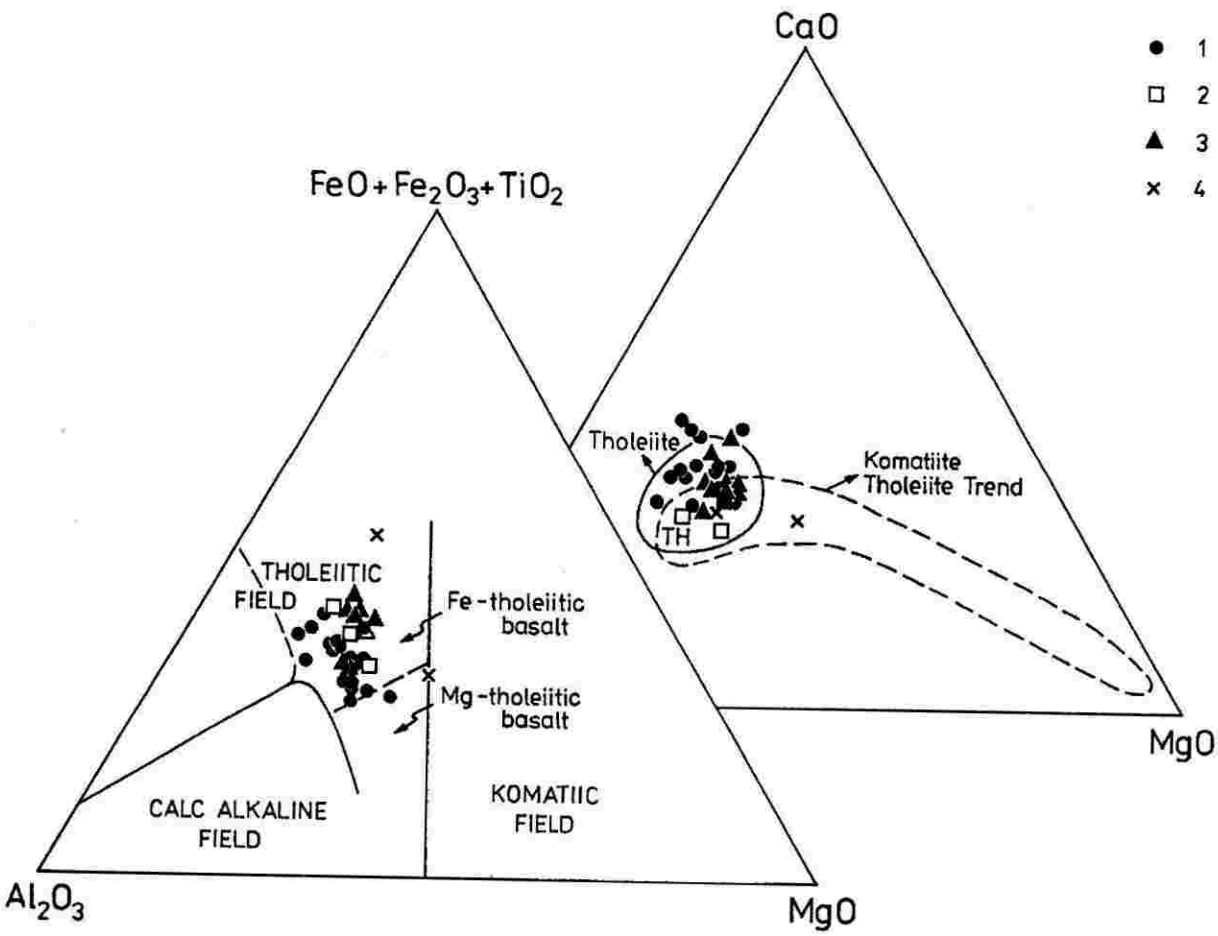

Figure 5a. Cation diagram of Jensen (1976) showing affinity of the metabasic rocks to tholeiites.
Figure 5b. CaO-Al_2O_3-MgO plot for all metabasic rocks. Compositional fields after Condie (1981). With an exception of the sample KH-22, all metabasic rocks fall into the tholeiite field.

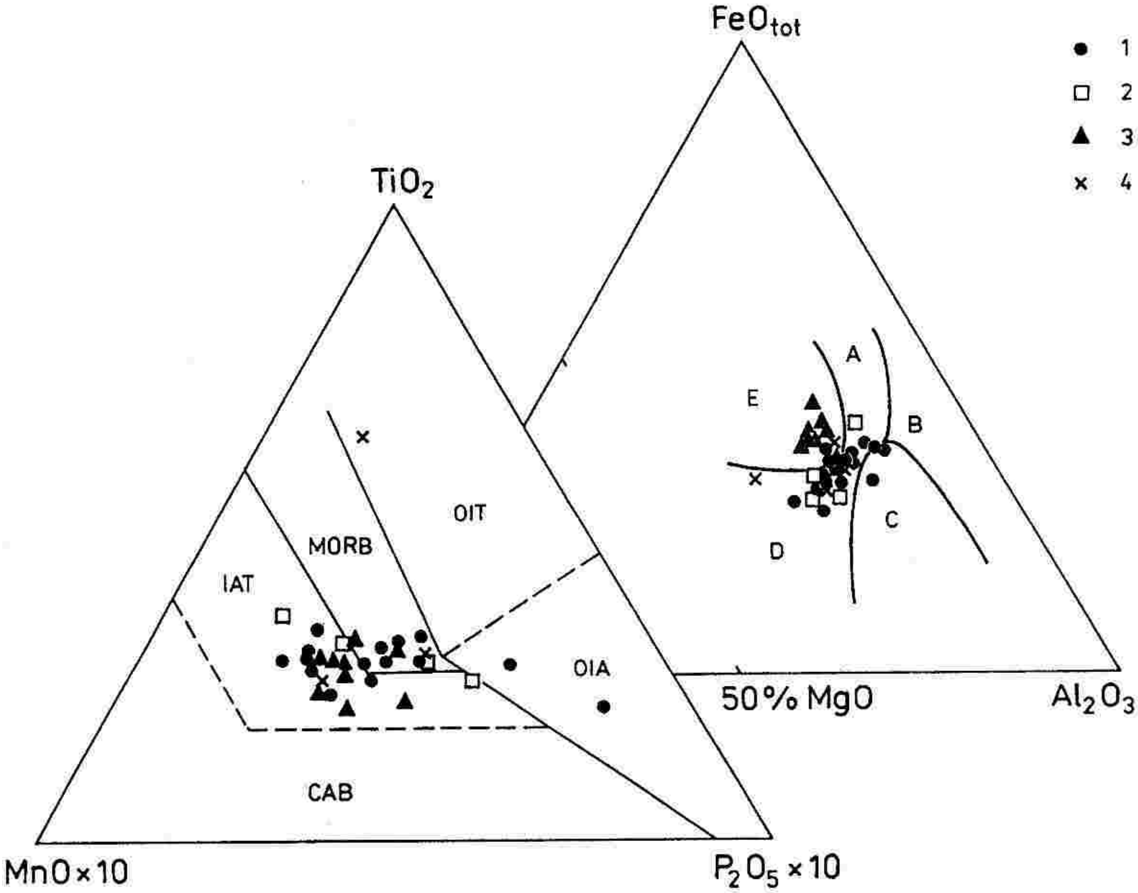

Figure 6a. The TiO_2-MnOx 10 -P_2O_5x 10 plot for analyzed metabasic rocks. Compositional fields after Mullen (1983). With an exception for the samples KH-13, KH-29, KH-30 (the OIA field) and for the sample KH-27 (the OIT field), all metabasic rocks fall into the MORB and the IAT fields.

Figure 6b. Discrimination diagram of Pearce et al.(1977) showing that most of samples fall into both the fields E and D. Fields: A=continental (KH-3, KH-8, KH-11, KH-12, KH-13, 14), B=spreading centres island, C=orogenic (KH-5, KH-9), D=ocean ridge and ocean floor basin, E=ocean island.

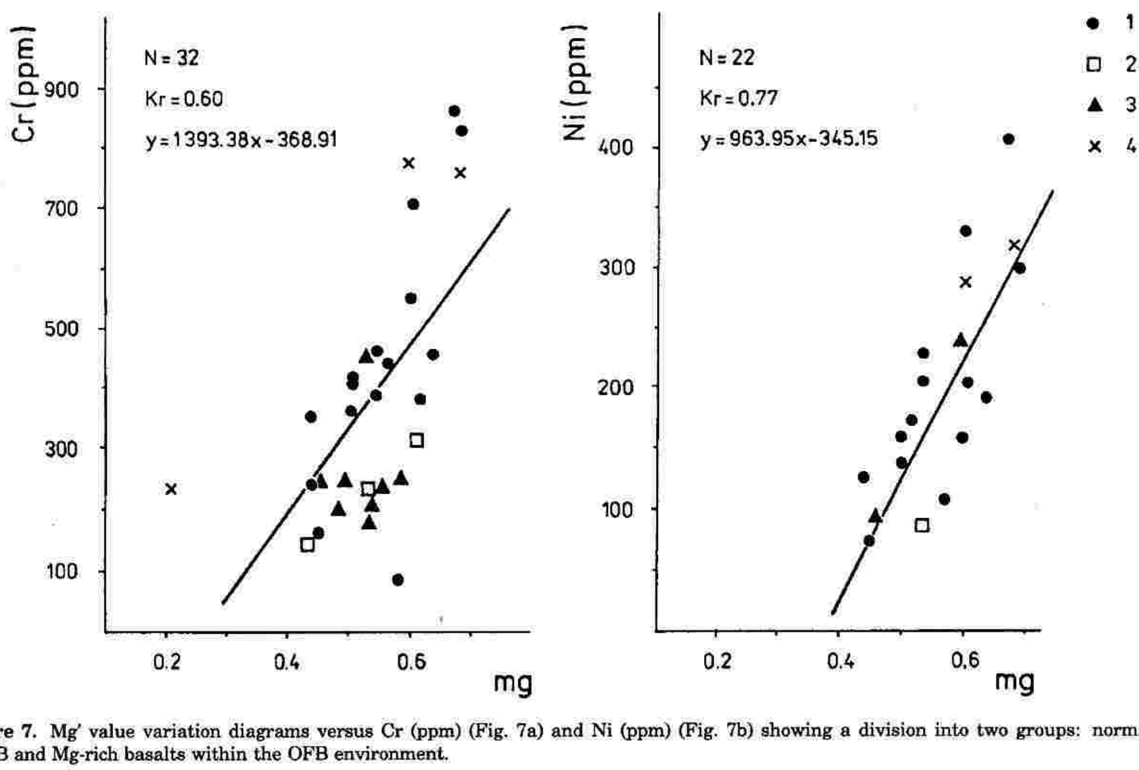

Figure 7. Mg' value variation diagrams versus Cr (ppm) (Fig. 7a) and Ni (ppm) (Fig. 7b) showing a division into two groups: normal-type MORB and Mg-rich basalts within the OFB environment.

Further chemical characteristics of the metabasic rocks is provided by the MnO × 10 – TiO_2 – P_2O_5 × 10 diagram after Mullen (1983) (Fig. 6a). With a few exceptions, most of the metabasic rocks can be compared with both the oceanic tholeiites (N-MORB or E-MORB) and the island-arc tholeiites (IAT) from the destructive plate margins. The garnetiferous amphibolite from Plaňany (KH-27) is located in the ocean-island tholeiite field (OIT). For the banded- and massive amphibolite (KH-13, KH-29, and KH-30), an affinity to the ocean-island alkali basalts (OIAB) is suggested. In general, volcanic islands like the Hawaiian Archipelago may contain both the tholeiitic and alkali basalts within volcanic sequences, however, island-arc series volcanoes are rather characterized by the explosive eruptions of basaltic andesites, rarely of basalts (Wilson 1993).

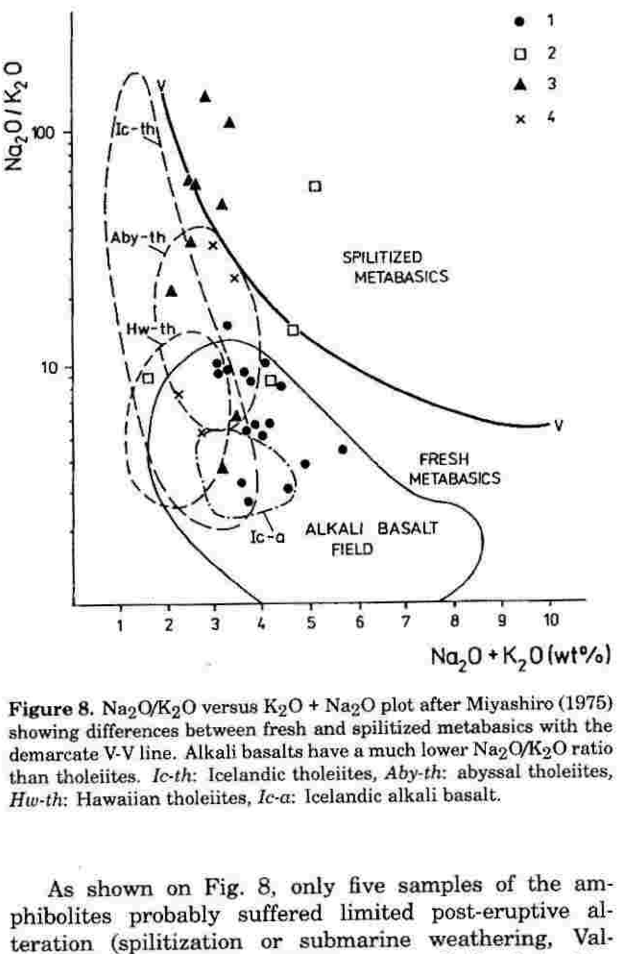

Figure 8. Na_2O/K_2O versus K_2O + Na_2O plot after Miyashiro (1975) showing differences between fresh and spilitized metabasics with the demarcate V-V line. Alkali basalts have a much lower Na_2O/K_2O ratio than tholeiites. *Ic-th*: Icelandic tholeiites, *Aby-th*: abyssal tholeiites, *Hw-th*: Hawaiian tholeiites, *Ic-a*: Icelandic alkali basalt.

As shown on Fig. 8, only five samples of the amphibolites probably suffered limited post-eruptive alteration (spilitization or submarine weathering, Vallance 1974). Miyashiro (1975) presented discrimination between altered and fresh basalts on a Na_2O / K_2O versus (Na_2O + K_2O) plot, in which the line V-V demarcates the altered basalts on its concave side.

An above discussed plots provide an useful way to display the compositional range; however, the metabasic rocks may differ from others in terms of their trace- and REE geochemistry.

Trace elements

Judging from their trace-element abundances normalized to MORB, *retrograded eclogite and diablastic amphibolite* of the Gföhl Unit (Fig. 9f) show a slightly flat pattern, typical of the MORB primitive tholeiite. With the exception of Sr, the incompatible elements of low-ionic potential (K, Rb, Ba, Th) are depleted (some below the MORB normalizing line, 1.0) and element ratios K / Ba and K / Rb are characteristically higher for them than for tholeiitic basalts generated in other tectonic environments. A further exception is that the moderately incompatible elements (P, Hf) are slightly enriched. The K / Ti ratios showing differences between the N-type and E-type MORB are lower than 0.20. The ferromagnesian elements such as Cr, Ni, Ti, and Sc (compatible with mafic constituents) are unfractioned. The plate tectonic setting of these rocks corresponds to a mid-ocean ridge environment. In addition, only the *least retrograded eclogite* (KH-32, Poličany) (Fig. 9e) exhibits a pattern representing ocean-island tholeiite and within-plate environment.

Rarely, some of the diablastic amphibolites show a tendency to E-type MORB pattern (Fig. 10e) similar to volcanites erupted in the vicinity of mantle hotspots (e.g. Galapagos spreading centre). All the incompatible elements from Sr to Th are less depleted and the ratio K / Ba is higher than that in N-MORB. The E-MORB pattern has chemical characteristics intermediate between those of N-MORB and those of the ocean island basalts (OIT). From the N-type MORB it is distinguishable by the ratio K / Ti higher than 0.20, although the Ti, Sc and Cr abundances have a steeper gradient. Thus the abundances of these elements should be useful indicators. The lower absolute abundances of most incompatible elements including Ta, Nb, Ce, P, Zr, Hf, Sm, Ti, Yb, Sc, and compatible ones such as Ni and Cr are significant in terms of the island-arc basalts (IAT) indicating that basalts might have been derived from fractionated magma (Pearce et al. 1977).

One sample of the *garnetiferous amphibolite* from the Plaňany Formation (KH-27), that contains higher amounts of K, Rb, and Ba, can be compared with the oceanic-island alkali basalt (OIAB) within intra-plate setting (WPB) because of its high TiO_2 content. The moderate P and Hf enrichment and the Cr depletion relative to MORB is apparent on figure 9d.

A further comparison with eclogites, retrograded eclogites and garnetiferous amphibolite of the Moldanubicum support the data given by Dudek-Fediuková (1978).

Massive amphibolite and some of the striped varieties from the Micaschist Zone represent island-arc tholeiites (IAT), an interpretation supported by the major component diagrams as well. Although the number of samples is fewer, the trace-element pattern (Fig. 9b) shows marked peaks at K and Rb, Th and Ta, P and to a lesser extent of Ti. Typical is the smaller amount of Ce, Hf, Sm, Sc, and Cr relative to N-MORB and more advanced fractionation.

In contrast, the somewhat higher Cr (235-468 ppm) and Ni (81-230 ppm) quantities and higher Mg' value indicating that less fractionated magma types are present in the samples of KH-3 (Český Šternberk), KH-5 (Paběnice), KH-14 (Markovice), and KH-31 (Víska) (Fig. 9c). These massive amphibolites collected in the Moldanubian Zone are transitional from an ocean island- to mid-ocean ridge setting. The trace-element pattern displays a broadly concave segment at Sr to Ta that emphasizes a slight enrichment above the MORB normalizing line. The other elements such as P, Hf, Sm, Ti, Sc, and Cr retain abundances close to unity.

The Mg-richer massive amphibolites (KH-20, KH-22) from the Plaňany Formation (Fig. 9a) possess much greater amounts of ferromagnesian elements such as Fe, Ni, and Cr, coupled with a higher Mg' value, and thus appear to be more indicative of an ocean-floor basalt than

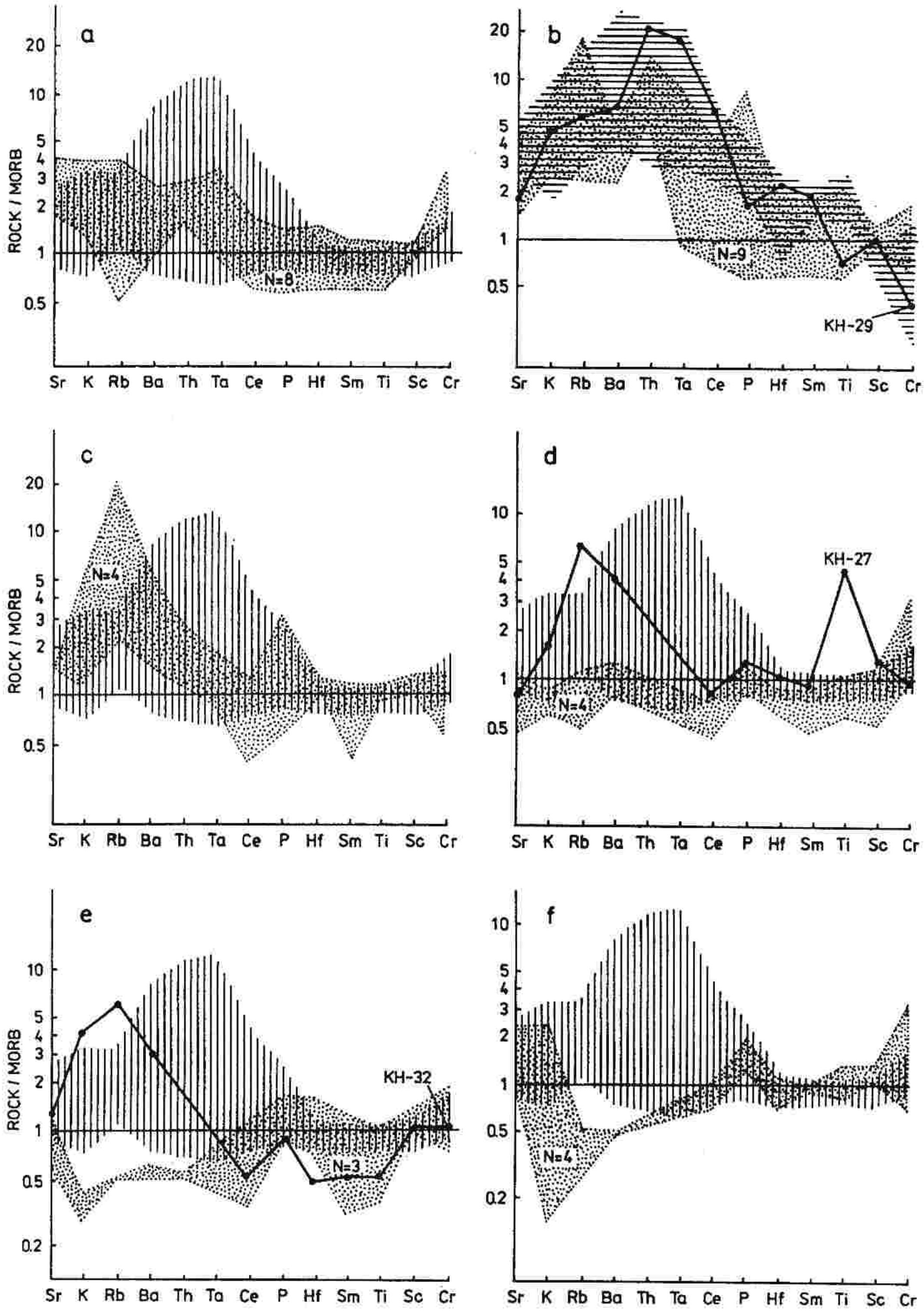

Figure 9a. Trace-element abundance normalized against a standard mid-ocean ridge basalt (N-MORB) for the retrograded eclogite (1-MORB normalized after Humphris et al. 1985, 2-MORB after Pearce 1982). The elements are ordered in sequence of descreasing incompability from left to right.

Figure 9b. Trace-element abundance normalized to MORB for the banded amphibolites (1-MORB normalized by Humphris et al. 1985, 2 -WPB normalized by Pearce 1982).

Figure 9c. Trace-element abundance normalized to MORB for the massive amphibolite of the Moldanubian Zone

Figure 9d. Trace-element abundance normalized to MORB for the garnetiferous amphibolite of the Plaňany Formation

Figure 9e. Trace-element abundance normalized to MORB for the retrograde eclogite and diablastic amphibolite of the Malín Formation.

Figure 9f. Trace-element abundance normalized to MORB for the retrograded eclogite of the Malín Formation.

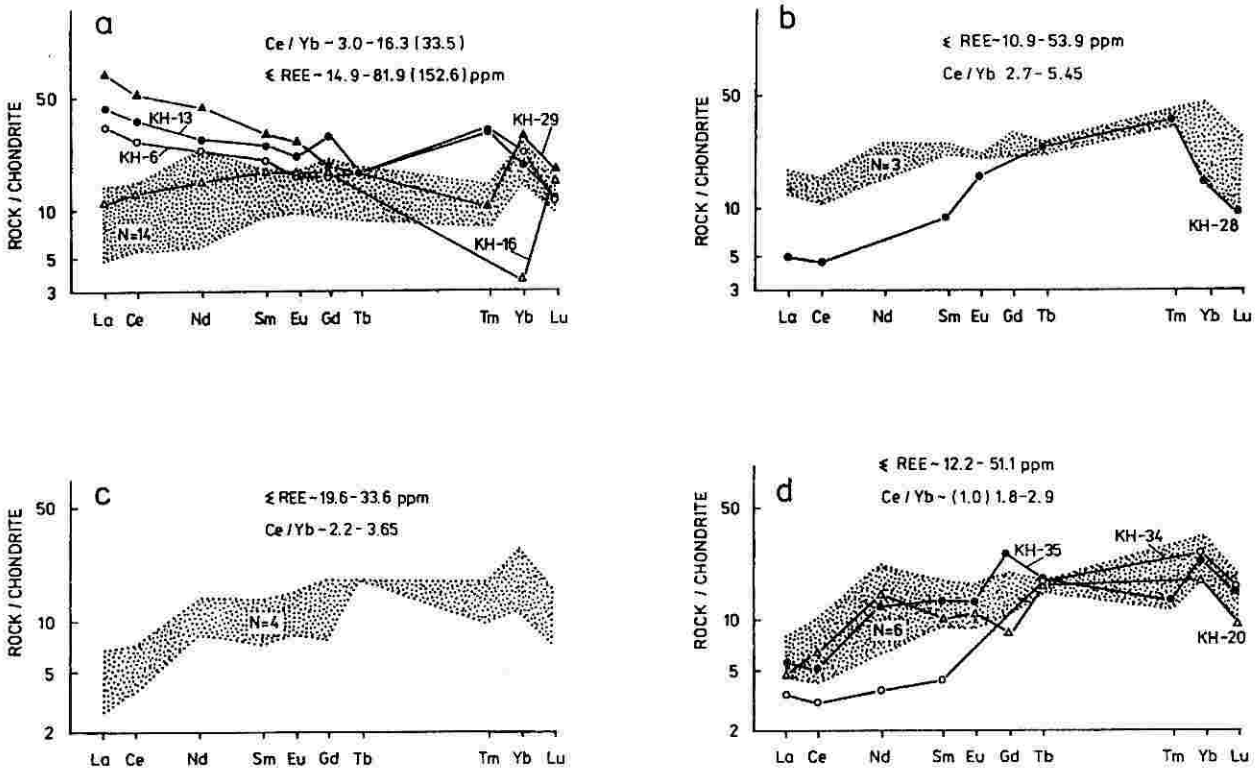

Figure 10a. Rare-earth element variation of the banded amphibolites of the Rataje Micaschist Zone (All analyses are normalized to chondrite according to Herrmann, 1970).
Figure 10b. Rare-earth element variation of the massive- and garnetiferous amphibolites from the Moldanubicum margin
Figure 10c. Rare-earth element variation of the massive amphibolite and the garnetiferous amphibolite from the Plaňany Formation
Figure 10d. Rare-earth element variation of the retrograded eclogite and the garnetiferous amphibolite from the Malín Formation.

normal-type MORB. The slight depletion of Sr, Rb and K,, and even depletion of Ce, Hf, Sm is apparent, while the amounts of P, Ba and Ti are mildly elevated.

The banded variety of amphibolite from the Micaschist Zone is divisible into two separate geochemical groups. In the first, the trace-element abundances are comparable to an ocean-island tholeiite (OIT), e.g. those in samples of KH-1 and KH-6. They represent an intra-plate environment (Fig. 9c). Compared to N-type MORB, the large-ion lithophile elements (LILE) such as K, Ba, and some of the large high-valency elements such as Th, Ce, Ta show relative enrichment, whereas transition metals (Cr,Ni) are slightly depleted. The Atlantic oceanic islands are well documented examples.

The second group (e.g. sample KH-29 in Fig. 9b) is, in general, enriched in incompatible elements (LILE) such as K, Rb, Ba and also in Th, Ta, Ce, and P, relative to MORB and OIT. The segment from Hf to Cr shows some depletion. Therefore, the transitional trend to alkali basalts and basanitoids (OIAB) within the ocean-island environment is evident. This is typical for certain volcanoes in islands of the Atlantic Ocean as noted Pearce (1982).

Rare earth elements

Total REE abundances are given in Appendix 4, Tables 1-3. Accompanying figures 10a through 10d present the chondrite –normalized REE patterns as an illustration for following metabasic rocks:

Retrograded eclogite and diablastic amphibolite. The REE patterns (in Fig. 10d) are in good agreement with the other chemical aspects of these rocks. The level of total REE abundances is relatively low and it ranges between 12.2 ppm and 51.1 ppm. Unfractionated heavy REE abundances and the flat-shaped REE profiles are most typical. All the patterns show considerable depletion of the light-REE [$(Ce / Yb)_N$ ratio between 0.37 and 0.59] like a primitive tholeiite occurring within mid-ocean ridge environment (N-MORB). This trend is shown for amphibolites from the Moldanubian Zone as well (Fig. 10b). The garnetiferous amphibolite (KH-28, Vlastějovice), which is weakly overprinted by migmatization, is different from the other samples in that it is more depleted in the LREE (La, Ce, Nd, Sm) as well as in the HREE (Lu and Yb,) relative to the Tb and Tm ;the total REEs content is only 9.9 ppm. The more LREE depletion in some samples, parallel to that of phosphorus, may be likely caused by alteration (e.g. spilitization).

The second type with less depleted LREE (convex shape from Ce to Sm), with [$(Ce/Yb)_N$ = 2.33] and an intermediate concave pattern from Gd to Yb, is consistent with E-MORB including the admixture of a plume component (e.g. sample KH-24). This pattern is evident in Figure 10 c for garnetiferous amphibolite of the Plaňany Formation.

Minor massive amphibolite s.s. and some of the striped amphibolites (with igneous-looking relics) usually have a similar level of the total REE contents as in the rocks mentioned above (21.6-55.3 ppm), although these rocks evidently originated under different metamorphic conditions. The REE patterns are flat-shaped (from Nd to Yb segment) with a less defined Eu-anomaly (Eu/Eu* = 0.52 -0.99) or with a moderate positive Eu-anomaly

(KH-5). The ratio $(Ce/Yb)_N$ varies between 0.38 and 1.1 owing to the apatite content (P_2O_5). The typically LREE depleted pattern as in the MORB and similarity in trace-element chemistry as in the IAT are the main reasons for regarding these rocks as an island-arc tholeiite.

Banded amphibolite. The total REEs content show a division into two groups: the majority of amphibolite samples with the low total value (ranging between 16.4 ppm and 30.9 ppm), and those with a high value ranging between 81.9 and 152.6 ppm.

In the first group, the REE patterns are less depleted in the LREE (La, Ce, Nd), and also enriched in Yb, while the segment from Sm to Tm is flat-shaped. The $(Ce / Yb)_N$ ratio ranges between 0.67 and 1.10 for amphibolites from the Micaschist Zone (KH-1, KH-2, KH-8, KH-9, KH-10, KH-11, KH-12, KH-15, KH-18). This combination of features has an analog in oceanic-island environment.

In the second, banded amphibolite with higher total REEs content (KH-13, KH-29) are characterized by slight to moderate fractionation of LREEs [$(Ce / Yb)_N$ between 1.10 and 3.28]. The sole exception is sample KH-13 that has a slightly higher amount of both Gd and Tm. The remaining patterns resemble those of ocean-island alkali basalt (OIAB). This may be a typical feature for transitional basalts erupted in islands in the ocean.

7. Conclusion

Based on microtextural relations and mineral chemistry data, the retrograded eclogite produced assemblages of grossularite –almandine, diablastic symplectites with an pargasitic hornblende and acid plagioclase after omphacite, and sometimes quartz. Original eclogitic rocks, which underwent various extents of re-equilibration in the granulite and amphibolite facies of metamorphism (e.g. O'Brien and Vrána 1995), are more frequent in the uppermost Gföhl Terrane, predominantly in both the Běstvina- and Malín Formations. Thermobarometric estimates and garnet composition provide a basis for comparion with other types of the Czech eclogite occurrences. The highest P-T estimations of equilibration are interpreted for the least retrograded eclogite from Poličany (KH-32) enclosed in the serpentinite body (equilibration at 20.1 kbar at 1008 °C), similar to the transitional types to HP-HT, group A Moldanubian eclogites (Beard et al. 1992). However, most obvious in the KHCC are the medium-temperature retrograde eclogite varieties (550-900 °C). This heterogeneity may have resulted from a former heterogenous mantle ca. 50 km beneath the present surface and from various degrees of eclogite recrystallization. Foliated garnetiferous amphibolites were completely recrystallized during a later granulite-facies overprint, and relics of high pressure assemblages are only known in the specimen of KH-35 (Žehušice). According to Graham and Powell (1984), P-T conditions of equilibration for this rock have been estimated at ca. 606 °C and at a pressure of 13.3 kb.

For massive amphibolites of the Moldanubian Zone, mineral assemblages and chemical compositions of coexisting phases indicate that equilibrium conditions were attained at upper amphibolite facies (KH-31 Víska, 7.3-8 kb, KH-8 Chedrbí, 8-9.7 kb at aprox. 550 °C). Petrographically and geochemically it is evident that diverse amphibolites from the Micaschist Zone are of another nature when high-pressure metamophic relics are lacking.

Whereas the above described rocks were subjected to a polymetamorphic evolution, most of the banded- and striped amphibolites in the Rataje Micaschist Zone mainly represent igneous basic rocks accompanied by metamorphism at the lower amphibolite facies. Banded amphibolites from the Micaschist Zone are estimated to have equilibrated at a minimum pressure of 5.0-6.2 kb and temperature of 530-570 °C. The episodic reactivation is at decreasing temperatures and pressures related to green-schist facies of metamorphism.

Geochemically, various retrograded eclogite and diablastic amphibolites in the crystalline sequence of the Malín Formation have a subalkaline MORB-like composition, with the exception of the slightly retrograded eclogite from Poličany (sample KH-32); it shows a pattern representing ocean-island tholeiite. In the Plaňany Formation, garnetiferous amphibolite (sample of KH-27) corresponds to oceanic-island alkali basalt.

Massive- and some of the striped amphibolites from the Micaschist Zone (predominantly with metagabbro relics) exhibit IAT-like immobile trace element characteristics. The metabasic bodies are traced at the present erosion level, mainly along the Sázava river area and also in the Mančice-Ratboř region (Koutek 1933, Kratochvíl 1952). Less fractionated magma types representing the Mg-rich massive amphibolite from the Plaňany Formation (KH-20, KH-22) and massive amphibolite from the northern margin of Moldanubian Zone must have originated either in an ocean-floor setting or in a mid-ocean ridge setting, respectively.

The whole-rock data and microchemistry emphasize two contrasting groups within the banded amphibolite:

(a) the first is plotted in the field of ocean-island tholeiite (Hawaiian type, WPA)
(b) the second comprises products of volcanism tending to alkaline basalts and basanitoids (OIAB).

The scenario outlined above implies a compressional tectonic regime. With respect to petrographic variability and mode of occurrence, regardless of the effect of deformation, this work presents further evidence for a multistage uplift history within the KHCC and provides useful information about metabasic rocks.

Acknowledgements

The study was funded by the Grant Agency of the Czech Republic, Grant No. 205 / 93 / 0341. Ing. J. Fiala, CSc. and RNDr. Fr. Patočka, CSc. are thanked for permitting the use of samples and to publish their analytical data. We are indebted to analysts M. Kozumplíková and Ing. A. Langrová from Geological Institute ASCR for their valuable help with microprobe work. The figures were redrawn by J. Rajlichová. Finally, we thank Dr. Prof. M. Malinky from the University of Maryland for comments on an earlier draft of the manuscript.

References

ANDERSON D.J. and LINDSLEY D.H. 1988. Internally consistent solution models for Fe-Mn-Ti oxides. *Amer. Mineralogist*, 73, 714-726.

BAILEY S.W. 1980. Summary of recommendations of AIPEA Nomenclature Committee on Clay Minerals. *Amer. Mineralogist*, 65, 1-7.

BEARD B.L., MEDARIS L.G., JOHNSON C.M., MÍSAŘ Z. and JELÍNEK E. 1991. Nd and Sr isotope geochemistry of Moldanubian eclogites and garnet peridotites, Bohemian Massif, Czechoslovakia. 2nd Eclogite Field Symposium, Spain, 1991. *Terra Nova*, 3, Suppl. 6, 4.

BEARD B.L., MEDARIS L.G. Jr., JOHNSON C.M., BRUCKNER H.K. and MÍSAŘ Z. 1992. Petrogenesis of Variscan high-temperature Group A eclogites from the Moldanubian Zone of the Bohemian Massif, Czechoslovakia. *Contrib. Mineral. Petrol.*, 111, 468-483.

BENEŠ K. *et al.* 1963. *Vysvětlivky k přehledné geologické mapě ČSSR 1:200 000, M-33-XXII Jihlava.* Nakl. ČSAV, Prague, (in Czech).

BLUNDY J.G. and HOLLAND T.J.B. 1990. Calcic amphibole equilibria and a new amphibole-plagioclase geothermometer. *Contrib. Mineral. Petrol.*, 104, 208-224.

BOHLEN S.R. and LIOTTA J.J. 1986. A barometer for garnet amphibolites and garnet granulites. *J. Petrology*, 27, 1025-1034.

BREY G.P., NICKEL K.G. and KOGARKO L. 1986. Garnet-pyroxene equilibria in the system CaO-MgO-Al_2O_3-SiO_2(CMAS): prospects for simplified ("T-independent") lherzollite barometry and eclogite barometer. *Contrib. Mineral. Petrol.*, 92, 448-455.

CARSWELL D.A. 1990. Eclogites and Eclogite Facies. In: Carswell, D.A.(ed.): *Eclogite facies rocks.* Blackie, Glasgow, 1-13.

CATHELINEAU M. and NIEVA D. 1985. A chlorite solid solution geothermometer. The Los Azufres (Mexico) geothermal system. *Contrib. Mineral. Petrol.*, 91, 235-244.

CONDIE K.C. 1982. *Plate tectonics and crustal evolution.* Pergamon Press, 310 pp., New York.

CULEK A. 1951. Svatokřížský shluk hlubinných basických hornin u Ronova n.D. *Rozpr. Čs. Akad. Věd, Tř. II*, 8, 1-25, (in Czech).

DUDEK A. 1971. Chemical composition of Moldanubian eclogites and their garnets. *Krystalinikum*, 7, 167-180.

DUDEK A. and FEDIUKOVÁ E. 1974. Eclogites of the Bohemian Moldanubicum, *N. Jb. Mineral, Abh.* 121, 2, 127-159.

DUDEK A. and FEDIUKOVÁ E. 1978. Contribution to the classification of the Moldanubian eclogites. *MS Faculty of Science, Charles University, Prague.* pp. 18, (in Czech).

DUDEK A. and FEDIUKOVÁ E. 1978. Trace elements of the Moldanubian eclogites. *N. Jb. Mineral., Abh.*, 130, 187-207.

ELLIS D.J. and GREEN D.H. 1979. An experimental study of the effect of Ca upon garnet-clinopyroxene Fe-Mg exchange equilibria. *Contrib. Mineral Petrol.*, 71, 13-22.

FEDIUKOVÁ E. and DUDEK A. 1977. Trace elements of the Moldanubian eclogites. *N. Jb. Mineral. Abh.*, 130, 3, 187-207.

FEDIUKOVÁ E. 1989. Eclogites in Czechoslovakia. *Krystalinikum*, 20, 27-48.

FIALA J. 1985. Bečváry W. of Kutná Hora. In: DUDEK A. and MÍSAŘ Z. (eds.): 2nd International Eclogite Conference-1985: Post-Excursion Guide, Czechoslovak Part, 48-52.

FIŠERA M. 1977. Geologie a petrografie kutnohorského krystalinika západně od Kolína. *Výzk. Práce Ústř. Úst. geol. v roce 1977*, 19-31, (in Czech).

FIŠERA M. 1981. Geologické a petrografické poměry okolí Plaňan. *Výzk. Práce, Ústř. Úst. geol.*, 26, 5-42, (in Czech).

FLOYD P.A. 1991 (ed.). *Oceanic Basalts.* Blackie, Glasgow-London, Van Nostrand Reinhold, 456 pp. New York.

GHENT E.D. and STOUT M.Z. 1986. Garnet-hornblende thermometry, $CaMgSi_2O_6$ activity, and the minimum pressure limits of metamorphism for garnet amphibolites. *J. Geology*, 94, 736-743.

GOROKHOV I.M., LOSERT J., VARSHAVSKAJA E.S., KUTJAVIN E.P., MELNIKOV N.N. and CHEKULOAJEV V.P. 1977. Rb-Sr geochronologija metamorficheskich porod vostochnoj chasti Cheskogo massiva (rajon Rudnych gor i prilegajushchej k nim chasti Czesko-Moravskoj vozvyshenosti). *Opyt korreljacii magmaticheskich i metamorficheskich porod.* Nauka, Moskva, 81-100, (in Russian).

GRAHAM C.M. and POWELL R. 1984. A garnet-hornblende geothermometer: calibration, testing and application to the Pelona Schist, southern California. *J. Metam. Petrology*, 2, 13-32.

HELLMAN P.L., SMITH R.E. and HENDERSON P. 1979. The mobility of the rare earth elements: evidence and implications from selected terrains affected by burial metamorphism. *Contrib. Mineral. Petrol.*, 71, 23-44.

HERRMANN A.G. 1970. Yttrium and lanthanides: abundances in cosmos, meteorites, tectites and lunar specimens. *In* WEDEPOHL K.H. (ed.): *Handbook of Geochemistry.* Springer Verl., 442 pp., Berlin-Heidelberg-New York.

HEY M.H. 1954. A new review of the chlorites. *Mineral. Magazine*, 30, 210.

HOLLAND T.J.B. 1979. Experimental determination of the reaction paragonite = jadeite + kyanite + H_2O, and internally consistent thermodynamic data for part of the system Na_2O-Al_2O_3-SiO_2-H_2O, with applications to eclogites and blueschists. *Contrib. Mineral Petrol.*, 68, 293-301.

HOLUB F.V. and MUNSHI R.L. 1984. Subsolidus reaction rims between olivine and calcic plagioclase in the Svatý Kříž Massif, Eastern Bohemia. *Krystalinikum*, 17, 47-58.

HUMPHRIS E.E., THOMPSON G., SCHILLING J.G. and KINGSLEY R.A. 1985. Petrological and geochemical variations along the Mid-Atlantic Ridge between 46 °S and 32 °S: influence in the Tristan da Cunha mantle plume. *Geochim. Cosmochim. Acta*, 49, 1445-1464.

IRVINE T.N. and BARAGAR W.R.A. 1971. A guide to the classification of the common volcanic rocks. *Can. J. Earth Sci.*, 8, 523 –548

JACOB D., JAGOUTZ E., LOWRY D., MATTEY D. and KUDRJAVTSEVA G. 1995. Diamondiferous eclogites from Siberia: Remnants of Archean oceanic crust. *Geochim. Cosmochim. Acta*, 58, 23, 5191-5207.

JAKEŠ P., JELÍNEK E., FIALA J. and TAYLOR S.R. 1994. Major and trace elements in "eclogite" and their host garnet peridotites, data from the Bohemian

Massif. In: V. BUCHA, BLÍŽKOVSKÝ, M. et al. (eds.): *Crustal Structure of the Bohemian Massif and the West Carpathians.* Academia Praha, 257-271.

JENSEN L.S. 1976. A new cation plot for classifying subalcalic volcanic rock. *Ontario Div. Mines, M.P.*, 66, 33 p.

JOANNY V., VAN ROERMUND H. and LARDEAUX J.M. 1991. The clinopyroxene/plagioclase symplectite in retrograde eclogites: a potential geothermobarometer. *Geol. Rundschau*, 80, 303-320.

KALIBA J. 1986. Geologické poměry kutnohorského krystalinika mezi Sanopšemi a Českým Šternberkem. *Diploma Thesis, Faculty of Science,* Charles University, Prague, (in Czech).

KLÁPOVÁ H. 1988. Retrogradní přeměna krušnohorských eklogitů. *Věst. Ústř. Úst. geol.*, 63, 1, 1-10, (in Czech).

KLÁPOVÁ H. 1990. Eclogites of the Bohemian part of the Saxothuringicum. *Rozpravy Čes. Akad. Věd, ř. matem.-přír. Věd,* 100, 5, 1-86.

KOHN M.J. and SPEAR F.S. 1989. Empirical calibration of geobarometers for the assemblage garnet + hornblende + plagioclase + quartz. *Amer. Mineralogist,* 74, 77-84.

KOUTEK J. 1933. Geologie posázavského krystalinika I. *Věst. Stát. Geol. Úst. ČSR,* 9, 6, 319-333, (in Czech).

KOUTEK J. 1939. Geologie posázavského krystalinika II (Oblast západně od Českého Šternberka). *Věst. Stát. Geol. Úst. ČSR,* 15, 57-68, (in Czech).

KOUTEK J. 1947. Krystalinikum ve východní a jižní části listu Kutná Hora. *Věst. Stát. Geol. Úst. ČSR,* 22, 119-121, (in Czech).

KOUTEK J. 1963. Metabazity, metatufy a metatufity v ratajské zóně v Posázaví. *Zpr. geol. Výzk. v Roce 1962*, 67-69, (in Czech).

KOUTEK J. 1965. Problémy kutnohorského krystalinika a přilehlého Posázaví. *Čas. Mineral. Geol.*, 10, 497-498, (in Czech).

KRATOCHVÍL F. 1934. Les prehnites des environs de Čáslav. *Bull. Int. d'l Acad. Sci. de Boheme,* 35 , 85-89.

KRATOCHVÍL F. 1947. Příspěvek k petrografii českého krystalinika *Sbor. Stát. geol. Úst. ČSR,* 14, 449-536, (in Czech).

KRATOCHVÍL F. 1952. O některých amfibolitech na listu speciální mapy Kutná Hora. *Sbor. Ústř. Úst. geol.*, 19, Odd. geol., 291-311, (in Czech).

LE BAS M.J., LE MAITRE R.W., STRECKEISEN A. and ZANETTIN B. 1986. A chemical classification of volcanic rocks based on the total alkali-silica diagram. *J. Petrology,* 27, 745-750.

LETERRIER J., MAURY R.C., THONON P., GIRARD D. and MARCAL M. 1982. Clinopyroxene composition as a method of identification of the magmatic affinities of paleo-volcanic series. *Eart Planet. Sci. Letters,* 59, 139-154.

LIOU J.G., KIM H.S and MARUYAMA S. 1983. Prehnite--epidote equilibria and their petrologic applications. *J. Petrology,* 24, 321-342.

LOSERT J. 1967. Contribution to the problem of the pre-Assyntial tectogenesis and metamorphism in the Moldanubicum of the Bohemian Massif. *Krystalinikum,* 5, 61-84.

MATTE Ph., MALUSKI H., RAJLICH P. and FRANKE W. (1990): Terrane boundaries in the Bohemian Massif: Result of large-scale Variscan shearing. *Tectonop ysics,* 177, 151-170.

MEDARIS L.G. Jr. 1985. Czech and Norwergian garnet peridotites and pyroxenites: application and evaluation of geothermometry. *Terra Cognita,* 5, 440.

MEDARIS L.G. Jr., BEARD B.L., MÍSAŘ Z. and JELÍNEK E. 1991. Czech eclogites in the Moldanubian Zone of the Bohemian Massif: petrological characteristics and tectonic significance. 2nd Eclogite Field Symposium, Spain, 1991. *Terra Nova,* Suppl. 6, 7-8.

MEDARIS L.G., JELÍNEK E. and MÍSAŘ Z. 1995. Czech eclogites: Terrane settings and implication for Variscan tectonic evolution of the Bohemian Massif. *Eur. J. Mineral.*, 7, 7-28.

MESSIGA B. and BETTINI E. 1990. Reactions behaviour during kelyphite and symplectite formation: a case study of mafic granulites and eclogites from the Bohemian Massif. *Eur. J. Mineral.*, 2, 125-144.

MÍSAŘ Z., DUDEK A., HAVLENA V. and WEISS J. 1983. *Geologie ČSSR I. Český masív,* Státní pedagog. Nakl., 336 pp., Prague, (in Czech).

MIYASHIRO A. 1974. Volcanic rocks series in island arcs and active continental margins. *Amer. J. Sci.*, 274, 321-355.

MIYASHIRO A. 1975. Classification, characteristics and origin of ophiolites. *J. Geology,* 83, 249-281.

MIYASHIRO A. and SHIDO F. 1975. Tholeiitic and calc - alkalic series in relation to the behaviours of titanium, vanadium, chromium and nickel. *Amer. J. Sci.*, 275, 265-277.

MORIMOTO N. 1988. Nomenclature of pyroxenes. *Mineral. Magazine,* 52, 535-550.

MOTTANA A. 1986. Crystal-chemical evaluation of garnet and omphacite microprobe analyses: Its bearing on the classification of eclogites. *Lit os,* 19, 3/4, 169-170.

MULLEN E.D. 1983. $MnO/TiO_2/P_2O_5$: a minor element discriminant for basaltic rocks of oceanic environments and its implications for petrogenesis. *Eart Planet. Sci. Letters,* 62, 53-62.

MUNSHI R.L. 1978. Metabasites and associated rocks in Ronov-Moravany area, Eastern Bohemia. *Acta Univ. Carol., Geologica, Kratoc víl Vol.*, 293-305.

MUNSHI R.L. 1981. Petrology of gabbro-amphibolite complex, Ronov-Moravany area, Eastern Bohemia. *Acta Univ. Carol., Geologica,* 19-33.

O'BRIEN P.J. and CARSWELL D.A. 1993. Tectonometamorphic evolution of the Bohemian Massif: evidence from high presssure metamorphic rocks. *Geol. Rundsc au,* 82, 531-555.

O'BRIEN P.J. and VRÁNA S. 1995. Eclogites with short--lived granulite facies overprint in the Moldanubian

Zone, Czech Republic: petrology, geochemistry and diffusion modelling of garnet zoning. *Geol. Rundsc au*, 84, 473-488.

OLIVERIOVÁ D. 1987. Geologicko-strukturní poměry pestré skupiny krystalinika v údolí Sázavy. *Doctoral T esis, Faculty of Science, Prague*, (in Czech).

OLIVERIOVÁ D. 1993. Ca-Al mica, margarite-its occurrences and metamorphic significance in micaschists from the Kutná Hora Crystalline Complex. *J. Czec . Geol. Soc.*, 38, 3/4, 209-213.

ONDŘEJ A. 1922. O amfibolitech středního Posázaví. *Čas. Muz. Král. Čes., Odd. přír.*, XCVI, 66-72, (in Czech).

ORLOV A. 1930. Hadec od Mladotic u Ronova nad Doubravkou. *Sbor. St. geol. Úst. ČSR*, 9, 96.

PEARCE J.A. 1975. Basalt chemistry used to investigate past tectonic environment on Cyprus. *Tectonop ysics*, 25, 41-67.

PEARCE J.A. 1982. Trace element characteristics of lavas from destructive plate boundaries. *In* THORPE R.S.(ed.): *Andesites*. John Wiley and Sons, 525-548, Chichester.

PEARCE J.A. and CANN J.R. 1973. Tectonic setting of basic volcanic rocks determined using trace element analyses. *Eart Planet. Sci. Letters*, 19, 290-300.

PEARCE J.A., GERMAN B.E. and BIRKETT T.C. 1977. The relationship between major element chemistry and tectonic environment of basic and intermediate volcanic rocks. *Eart Planet. Sci. Letters*, 36, 121-136.

PEARCE J.A. and NORRY M.J. 1979. Petrogenetic implications of Ti, Zr, Y, and Nb variations in volcanic rocks. *Contrib. Mineral. Petrol.*, 69, 33-47.

PLYUSNINA L.P. 1982. Geothermometry and geobarometry of plagioclase-hornblende bearing assemblages. *Contrib. Mineral. Petrol.*, 80, 140-146.

POUBA Z., FIALA J. and PADĚRA K. 1987. Granulitový masiv u Běstviny v Železných horách. *Čas. Mineral. Geol.*, 32, 73-78, (in Czech).

POVONDRA P. and ŽÁČEK K. 1991. Krystalochemie minerálů skarnu z Vlastějovic nad Sázavou. *Acta Univ. Carol., Geologica*, 1/2, 71-101, (in Czech).

POWELL R. 1985. Regression diagnostics and robust regression in geothermometer/geobarometer calibration: the garnet –clinopyroxene geothermometer revised. *J. Metamorp . Geology*, 3, 321-243.

RAITH M. 1976. The Al-Fe (III) epidote miscibility gap in a metamorphic profile through the Penninic Series of the Tauern Window, Austria. *Contrib. Mineral. Petrol.*, 57, 99-117.

RYBURN R., R˚AHEIM A. and GREEN D.H. 1976. Determination of the P, T paths of natural eclogites during metamorphism-record of subduction: A correction to a paper by R˚aheim and Green (1975). *Lit os*, 9, 161-164.

SHIMIZU N. and ARCULUS R.J. 1975. Rare earth element concentrations in a suite of basanitoids and alkali olivine basalts from Grenada, Lesser Antilles. *Contrib. Mineral. Petrol.*, 50, 231 –240.

SCHMÄDICKE E., OKRUSCH M. and SCHMIDT W. 1992. Eclogite-facies rocks in the Saxonian Erzgebirge,Germany: high pressure metamorphism under contrasting P – T conditions. *Contrib. Mineral. Petrol.*, 110, 226-241.

SCHUMACHER J.C. 1991. Empirical ferric iron corrections: necessity, assumptions, and effects on selected geothermometers. *Mineral. Magazine*, 55, 3-18.

SOKOL R. 1925. Geologie okolí Kutné Hory. *Sborník Vlastiv. statí o politickém okrese kutno orském*, 5-40, (in Czech).

SPENCER K.J. and LINDSLEY D.H. 1981. A solution model for coexisting iron-titanium oxides. *Amer. Mineralogist*, 66, 1189-1201.

SUN S.S., NESBITT R.W. and SHARASKIN A.Ya, 1979. Chemical characteristics of mid-ocean ridge basalts. *Eart Planet. Sci. Letters*, 44, 119-138.

SYNEK J. 1991. Formation of sheath folds and reorientation of lineations in the western part of the Kutná Hora Crystalline Unit. *Věst. Ústř. Úst. geol.*, 66, 75-78.

SYNEK J. and OLIVERIOVÁ D. 1993. Terrane character of the north-east margin of the Moldanubian Zone: the Kutná Hora Crystalline Complex, Bohemian Massif. *Geol. Rundsc au*, 82, 566-582.

VALLANCE T.G. 1974. Spilitic degradation of a tholeiitic basalt. *J. Petrology*, 15, 1, 71-96.

WALSHE J.L. 1986. A six-component chlorite solid solution model and conditions of chlorite formations in hydrothermal and geothermal systems. *Econ. Geology*, 81, 681-703.

WEISS Z. and ĎUROVIČ S. 1983. Chlorite polytypism II. Classification and X-ray identification of trioctahedral polytypes. *Acta Crystallogr.*, B 39, 552-557.

WILSON M. 1993. *Igneous Petrogenesis: A Global Tectonic Approac* . Chapman and Hall, 466 pp., London, Glasgow, New York, Tokyo, Melbourne, Madras.

WOOD D.A., JORON J.L. and TREUIL M. 1979. A reappraisal of the use of trace elements to classify and discriminate between magma series erupted in different tectonic settings. *Eart Planet. Sci. Letters*, 45, 326-336.

Appendix 1
Modal composition of the mafic rocks

LIST OF SAMPLES

KH-1 Čekanov, 3.5 km NE of Sázava n. S., banded amphibolite
KH-2 Ledečko, 2 km NW of Rataje n. S., banded amphibolite
KH-3 Český Šternberk, quarry N of village, massive amphibolite
KH-4 Kácov, garnetiferous amphibolite, slightly migmatitized
KH-5 Paběnice, SW of the town of Čáslav, banded amphibolite
KH-6 Třebonín, SW of Čáslav, banded amphibolite
KH-8 and KH-9 Chedrbí, SW of Čáslav, banded amphibolite, altered and interbedded in biotite-sillimanite quartzite
KH-10 Kluky, 3 km W of Čáslav, banded amphibolite
KH-11 Čáslav, quarry in vicinity, banded amphibolite with clinopyroxene
KH-12 Žleby, outcrop near village, banded amphibolite
KH-13 Okřesaneč, SE of Čáslav, small quarry, banded amphibolite
KH-14 and KH-15: Markovice quarry, banded amphibolite
KH-16 Markovice, outcrop in vicinity, diablastic amphibolite
KH-17 and KH-18: Malešov, abandoned pit, banded amphibolite
KH-19 Kbílek, 1st small quarry, 6 km S of the town of Kolín, striped amphibolite with clinopyroxene relics
KH-20 Kbílek, 2nd small quarry, massive amphibolite
KH-21 Mančice, 9 km SW of Kolín, small quarry at hill "Na skalce", retrograded eclogite
KH-22 Mančice, small quarry "Na skalce", massive pyroxene amphibolite
KH-23 Mančice, small quarry "Na skalce", retrograded eclogite
KH-24 and KH-25: Libodřice, 8.5 km WSW of Kolín, retrograded eclogite
KH-26 Libodřice, outcrop near village, diablastic amphibolite
KH-27 Plaňany, 12 km W of Kolín, large quarry, garnetiferous amphibolite from boudins in the sillimanite-biotite migmatite
KH-28 Vlastějovice n.Sázavou, large quarry on the Fiolík hill, garnetiferous amphibolite, slightly migmatitized
KH-29 and KH-30: Hodkov, 6 km NNE of Zruč n. Sázavou, outcrops of banded amphibolite
KH-31 Víska near Chotěboř, outcrop in the vicinity, massive amphibolite
KH-32 Poličany, S of Kutná Hora, outcrop of eclogite
KH-33 and KH-34: Poličany, outcrop of diablastic amphibolite
KH-35 Žehušice, 6 km N of Čáslav, outcrop of garnetiferous amphibolite

Table 1a
Modal composition of the mafic rocks from the Gföhl Unit (vol. %)

	KH-21	KH-23	KH-24	KH-25	KH-26	KH-32	KH-33	KH-34	KH-35
	Malín Formation								
symplectite Am+Pl	10.53	2.83	–	–	–	–	15.41	42.40	–
symplectite Cpx+Pl	0.65	–	–	1.75	0.11	0.01	2.32	7.90	–
hornblende	–	–	68.54	–	–	–	–	–	72.90
ferroedenitic hornblende	46.83	–	–	–	–	–	–	–	–
Fe-pargasite	–	62.30	–	63.75	47.68	76.06	37.52	25.04	0.20
clinopyroxene	–	–	–	–	–	–	–	–	–
garnet(Grs-Alm)	14.30	12.66	–	12.93	–	0.56	24.79	17.13	1.34
biotite	–	–	–	–	–	0.11	–	0.11	–
clinozoisite-epidote	1.06	0.23	–	0.06	21.28	0.11	3.25	0.17	–
ilmenite	0.21	0.14	0.53	0.14	0.35	–	1.79	1.10	0.40
calcite	0.14	tr.	0.02	0.35	0.30	–	0.02	2.64	–
plagioclase An_{07-13}	19.74	4.43	–	–	–	–	–	–	–
plagioclase An_{35-40}	–	–	23.32	7.58	9.52	20.00	0.03	0.45	14.95
quartz	5.33	13.18	2.90	12.61	11.59	1.34	14.43	0.12	8.40
secondary chlorite	0.17	–	–	–	–	0.11	0.02	0.12	–
sericite + kaolinite	–	0.33	0.31	0.16	7.70	1.19	–	1.00	–
kaolinite	0.43	–	–	–	–	–	–	–	0.10
hematite + goethite	–	–	–	–	–	–	0.01	0.30	–
accessory sphene	0.50	1.74	2.73	0.65	1.02	0.27	tr.	0.01	1.47
rutile	–	–	–	–	–	–	–	0.04	–
apatite	–	–	–	–	0.05	–	–	–	0.09
zircon	–	–	–	–	–	–	–	–	0.11
holes	–	2.15	1.65	–	–	–	–	–	–
total	99.98	99.99	100.00	99.98	100.00	99.98	99.98	99.99	100.00
number of points	4 150	4 240	4 170	6 320	3 730	5 415	5 590	3760	4 490

Explanations:

KH-21 and KH-23: retrograded eclogite, Mančice, quarry "Na skalce"
KH-24 and KH-25: retrograded eclogite, Libodřice
KH-26: eclogitic amphibolite, Libodřice,
KH-32: slightly retrograded eclogite, Poličany
KH-33 and KH-34: eclogitic amphibolite, Poličany
KH-35: garnetiferous amphibolite, Žehušice

Table 1b
Modal composition of the mafic rocks from the Gföhl Unit (vol. %)

	KH-19	KH-20	KH-22	KH-27	Pl-2	Pl-83
	Plaňany Formation					
hornblende	–	–	58.80	–	55.5	43.2
ferroedenitic hornblende	84.45	81.24	–	–	–	–
Fe-pargasite	–	–	–	59.14	–	–
clinopyroxene	0.55	–	21.50	–	–	–
garnet	–	–	–	4.15	–	1.1
biotite	–	–	–	0.50	3.4	23.4
clinozoisite-epidote	4.22	0.21	–	–	–	–
ilmenite	0.19	0.68	0.02	9.86	–	–
K-feldspar	tr.	–	–	–	–	–
plagioclase An_{07-13}	–	–	8.91	–	–	–
plagioclase An_{35-40}	8.20	14.26	–	13.64	32.3	19.9
quartz	0.43	1.18	9.53	12.44	–	10.5
secondary chlorite	–	–	–	–	–	–
sericite + kaolinite	0.58	1.25	0.86	0.02	–	–
calcite	0.43	0.02	–	–	–	–
scapolite	0.05	–	–	–	–	–
hematite + goethite	–	0.02	–	–	–	–
accessory sphene	0.77	0.68	–	0.02	6.2	1.4
leucoxene	–	–	–	0.02	–	–
rutile	0.13	0.34	0.02	–	0.4	–
apatite	–	–	0.06	0.20	tr.	–
zircon	–	–	0.06	–	–	–
pyrite	–	–	–	–	2.2	0.5
holes	–	0.11	0.24	–	–	–
total	100.00	99.99	100.00	99.99	100.0	100.0
number of points	6 210	4 540	4 650	5 920		

Explanations:

KH-19: striped amphibolite with clinopyroxene relics, Kbílek
KH-20: massive amphibolite, Kbílek,
KH-22: massive amphibolite from the outcrop "Na skalce", Mančice
KH-27: garnetiferous amphibolite from the quarry near Plaňany
Pl-2: amphibolite from the quarry of Plaňany (Fišera 1981)
Pl-83: garnetiferous amphibolite, biotitized, Plaňany (Fišera 1981)

Table 2 a
Modal composition of the mafic rocks from the Micaschist Zone (vol. %)

	KH-1	KH-2	KH-5	KH-6	KH-8	KH-9	KH-10	KH-11	KH-12	KH-13	KH-14	KH-15
Fe-hornblende	78.30	64.84	50.86	43.12	–	–	50.01	59.68	62.26	–	58.44	51.22
edenitic hornblende	–	–	–	tr.	44.47	39.83	–	–	–	–	–	5.05
pargasitic hornblende	–	–	–	–	–	–	–	–	–	42.27	–	–
clinopyroxene	–	0.05	–	–	3.89	–	0.11	11.70	–	–	–	–
garnet	–	–	–	–	–	–	–	–	–	–	0.13	–
biotite	–	–	–	–	–	–	–	–	tr.	–	–	–
clinozoisite-epidote	–	2.09	0.20	–	11.80	34.05	4.32	2.10	2.38	11.48	9.92	5.73
calcite	–	7.37	0.35	0.38	3.22	1.58	3.99	9.34	–	0.05	0.59	0.27
plagioclase An_{20-34}	–	–	–	–	–	–	–	–	–	43.50	–	–
plagioclase An_{35-38}	17.05	–	27.43	45.95	20.40	19.11	–	4.04	31.80	–	26.13	–
plagioclase An_{50-60}	–	–	–	–	–	–	–	–	–	–	–	34.77
plagioclase An_{70-80}	–	20.57	–	–	–	–	37.31	–	–	–	–	–
quartz	1.10	3.07	0.17	7.27	6.20	1.60	3.25	9.70	0.41	0.95	1.18	0.43
scapolite	–	–	–	–	tr.	–	–	2.49	–	–	–	–
ilmenite(leucoxene)	0.55	tr.	–	1.25	2.30	–	0.02	–	–	0.04	0.02	–
secondary chlorite	–	–	–	0.35	–	0.88	–	0.02	–	–	0.02	0.02
sericite + kaolinite	2.62	1.46	6.09	1.30	7.15	1.99	0.58	0.50	–	1.33	–	–
kaolinite	–	–	–	–	–	–	–	–	0.24	–	0.85	1.09
hematite + goethite	–	–	–	–	–	–	–	–	–	0.04	–	–
accessory sphene	0.36	0.55	2.37	0.31	0.56	0.09	0.29	0.35	2.04	0.25	2.13	1.38
rutile	0.02	–	–	–	–	–	–	–	–	–	0.02	–
apatite	–	–	–	0.05	–	0.02	–	–	0.53	0.04	0.02	–
zircon	–	–	–	–	–	–	–	–	0.17	–	0.20	–
pyrite	–	–	–	–	–	0.09	–	–	–	–	–	–
magnetite	–	–	–	–	–	–	–	–	0.05	–	–	–
holes	–	–	–	–	–	0.75	0.11	–	0.10	0.04	0.36	–
total	100.00	100.00	99.99	99.98	99.99	99.99	99.99	99.99	99.98	99.99	99.99	100.00
number of points	4 730	3 980	4 550	4 240	3 910	4 430	4 490	4 335	4 120	4 445	3 890	4 855

Explanations:

KH-1: banded amphibolite, Čekanov; KH-2: banded amphibolite with epidote, Ledečko; KH-5: banded amphibolite, Paběnice; KH-6: banded amphibolite, Třebonín; KH-8: banded amphibolite altered from Chedrbí (accompanied by the biotite-sillimanite quartzite; KH-7), KH-9: banded amphibolite with epidote, Chedrbí; KH-10: banded amphibolite with calcite-epidote bands, Kluky; KH-11: banded pyroxene amphibolite, slightly scapolitized, Čáslav; KH-12: banded amphibolite, Žleby; KH-13: banded amphibolite, Okřesaneč; KH-14 and KH-15: banded amphibolite with epidote, Markovice

Table 2 b
Modal composition of the mafic rocks from the Micaschist Zone (vol. %)

	KH-16	KH-17	KH-18	KH-29	KH-30
symplectite Cpx + Pl	0.75	–	–	–	–
hornblende	–	–	1.50	–	–
ferroedenitic hornblende	–	71.37	74.47	64.75	76.37
pargasitic hornblende	63.40	–	–	–	–
clinopyroxene	–	0.46	0.36	–	–
garnet	–	–	0.10	–	–
biotite	–	–	–	–	–
clinozoisite (Ps_{18})	8.15	1.11	3.20	2.19	0.11
ilmenite (leucoxene)	–	0.20	0.08	0.34	2.18
calcite	0.09	0.18	–	0.04	0.04
plagioclase An_{30-45}	24.35	23.47	15.86	23.14	12.04
quartz	0.21	1.32	2.75	1.12	0.15
secondary chlorite	0.04	0.12	–	0.27	0.53
sericite + kaolinite	0.28	–	–	7.29	5.44
kaolinite	–	0.93	0.35	–	–
accessory sphene	2.42	0.73	0.95	0.53	3.11
rutile	–	0.02	0.08	–	–
apatite	–	0.04	0.10	–	0.02
zircon	–	0.02	0.02	–	–
magnetite	–	0.20	–	–	–
holes	0.28	0.03	0.16	0.33	–
total	99.99	100.00	99.98	100.00	99.99
number of points	4 290	5 580	4 760	4 470	4 500

Explanations:

KH-16: diablastic amphibolite, Markovice near Čáslav
KH-17 and KH-18: banded amphibolite, Malešov
KH-29 and KH-30: banded amphibolite altered, Hodkov

Table 3
Modal composition of the mafic rocks from the Moldanubicum (vol.%)

	KH-3	KH-4	KH-28	KH-31
hornblende	61.85	–	–	–
pargasitic hornblende	–	–	–	70.64
ferroedenitic hornblende	–	56.66	59.31	–
clinopyroxene	0.13	0.06	–	–
garnet	–	1.61	–	–
biotite	–	tr.	–	–
clinozoisite-epidote	0.06	–	0.72	0.02
muscovite	–	–	0.19	–
ilmenite	1.00	1.05	0.08	2.11
plagioclase An_{07-35}	32.93	–	10.57	24.92
plagioclase An_{35-40}	–	24.51	–	–
quartz	0.58	7.16	0.33	0.75
secondary chlorite	0.44	0.17	9.86	0.07
kaolinite + sericite	2.07	8.55	15.14	1.48
goethite	0.31	–	0.02	–
calcite	–	–	1.70	–
accessory sphene	0.55	0.08	0.13	–
leucoxene	0.02	–	0.42	–
rutile	0.04	–	–	–
apatite	–	tr.	–	–
zircon	0.02	0.01	–	–
magnetite	–	0.10	–	–
holes	–	0.04	1.07	–
total	100.00	100.00	99.98	99.99
number of points	4 500	4 540	4 750	3 990

Explanations:

KH-3: massive amphibolite, Český Šternberk
KH-4: slightly migmatized garnetiferous amphibolite, Kácov
KH-28: slightly migmatized amphibolite, Vlastějovice
KH-31: massive amphibolite, Víska near Chotěboř

Appendix 2
Whole-rock chemical analyses

Table 1
Selected analyses of various mafic rocks from different units (wt %)

	NE margin of Moldanubicum				the Gföhl Unit – Malín Formation								
	massive amphibolite		Gt. amphibolite		retrograded eclogite					diablastic amph.			Gt. amphib.
	KH-3	KH-31	KH-4	KH-28	KH-21	KH-23	KH-24	KH-25	KH-32	KH-34	KH-26	KH-33	KH-35
SiO_2	48.16	47.32	51.08	44.72	50.55	48.26	47.32	47.82	48.53	44.50	46.16	49.81	48.84
TiO_2	1.43	1.36	1.44	1.81	1.58	1.59	1.68	1.97	0.83	0.53	1.53	0.88	1.04
Al_2O	14.63	15.88	14.42	16.65	14.11	14.20	14.08	14.03	15.01	14.82	14.15	15.44	14.82
Fe_2O_3	2.20	3.99	2.44	2.44	2.16	2.15	3.00	2.21	1.81	2.88	3.22	2.47	3.99
FeO	9.16	6.41	9.70	10.08	9.95	10.50	9.55	11.42	8.56	10.69	9.56	8.10	8.63
MnO	0.19	0.15	0.19	0.16	0.24	0.25	0.25	0.22	0.17	0.25	0.19	0.18	0.18
MgO	7.49	9.19	5.24	7.20	7.03	6.57	8.19	6.49	8.22	8.55	6.86	7.58	8.06
CaO	10.00	8.81	8.00	11.57	8.77	10.67	10.68	10.82	11.19	12.24	12.88	11.79	11.60
Na_2O	3.81	4.41	4.28	1.41	3.30	3.02	3.28	2.78	2.53	2.46	3.03	2.47	2.46
K_2O	0.44	0.31	0.82	0.16	0.13	0.49	0.03	0.02	0.65	0.04	0.06	0.04	0.07
P_2O_5	0.07	0.19	0.13	0.36	0.15	0.14	0.17	0.22	0.10	0.09	0.14	0.13	0.19
CO_2	0.08	0.15	0.27	0.36	0.25	0.11	0.18	0.15	0.17	1.23	0.55	0.11	0.44
H_2O^+	1.37	1.59	1.41	–	0.70	0.48	1.17	0.91	1.58	1.01	1.17	1.00	1.30
H_2O^-	0.37	0.18	0.23	0.36	0.19	0.22	0.19	0.21	0.34	0.17	0.20	0.14	0.11
Total	99.40	99.94	99.65	97.29	99.11	98.65	99.72	99.27	99.89	99.46	99.64	100.09	100.93

Microchemistry (ppm)

Cr	235	318	142	200	25	n.d.	182	245	260	454	202	238	210
Sc	48.6	40.8	42.9	55.4	49.3	n.d.	51.0	53.6	41.9	44.1	51.4	39.2	43.3
Ni	81	n.d.	n.d.	n.d.	n.d.	n.d.	n.d.	96	n.d.	n.d.	n.d.	n.d.	n.d.
Ba	52	29	28	123	25	<10	<10	<10	64	12	<10	11	10
Rb	4.5	4.5	37.1	44.1	2.3	<1	<1	<1	12.4	<1	<1	<1	<1
Sr	190	180	180	181	125	101	112	112	146	78	271	147	123
Th	n.d.	n.d.	0.58	n.d.	n.d.	n.d.	n.d.	n.d.	n.d.	n.d.	n.d.	n.d.	n.d.
Hf	2.55	2.51	3.22	2.52	l.64	2.12	n.d.	2.55	3.22	4.25	2.38	1.13	2.06
Ta	n.d.	n.d.	0.16	<1	n.d.	n.d.	n.d.	n.d.	n.d.	n.d.	n.d.	n.d.	n.d.

REE concentrations (ppm)

La	3.6	5.0	4.5	1.5	2.2	–	2.2	2.2	12.5	1.5	3.40	1.9	2.3
Ce	8.5	12.2	11.3	3.8	7.4	–	6.8	10.0	5.0	3.5	11.7	4.6	5.7
Nd	n.d.	13.5	12.0	n.d.	n.d.	–	n.d.	17.4	17.5	9.4	17.3	4.7	9.4
Sm	3.22	3.83	3.92	1.34	2.86	–	3.11	3.02	1.70	3.01	4.05	2.03	3.01
Eu	1.19	1.23	1.32	0.90	1.12	–	1.20	1.11	0.71	1.09	1.49	0.75	1.09
Gd	n.d.	14.14	5.98	n.d.	5.05	–	5.52	3.53	7.86	7.65	5.95	n.d.	7.65
Tb	0.84	<1	0.88	<1	<1	–	<1	<1	<1	–	<1	<1	<1
Tm	1.02	n.d.	0.90	0.88	0.63	–	0.46	0.45	0.55	0.47	1.02	0.50	0.47
Yb	2.51	2.24	4.11	1.29	3.66	–	3.56	3.41	1.96	3.12	4.46	2.22	3.12
Lu	0.74	0.47	0.68	0.23	0.54	–	0.59	8.53	0.37	0.58	0.72	0.41	0.58
E REE	21.62	52.61	45.59	9.94	23.46	–	23.44	41.65	38.15	30.32	50.09	17.11	33.32
$(Ce/Yb)_N$	0.38	1.10	0.55	0.59	0.41	–	2.33	0.59	0.51	0.21	0.53	0.42	0.37
$(Ce/Sm)_N$	0.56	3.2	0.68	0.60	0.55	–	0.46	0.70	0.62	0.80	0.61	0.21	0.40
Eu/Eu^*	0.99	0.52	0.93	0.92	1.00	–	0.98	1.13	0.57	(0.5)	1.03	1.85	0.75

Table 2
Selected analyses of various mafic rocks from different units (wt %)

	Plaňany Formation				the Rataje Micaschist Zone						
	gt. amphibolite/massive amphibolite				diablastic amphibolite			striped and banded amphibolite			
	KH-27	KH-22	KH-19	KH-20	KH-16	KH-17	KH-18	KH-14	KH-15	KH-5	KH-12
SiO_2	42.27	48.43	44.99	46.36	46.30	46.32	46.77	47.07	46.77	45.88	47.14
TiO_2	7.30	0.99	0.92	1.21	1.81	1.14	1.31	1.57	1.54	0.91	1.52
Al_2O_3	18.86	12.72	15.63	14.16	15.52	15.68	15.05	15.71	15.54	16.37	15.59
Fe_2O_3	1.93	2.23	1.98	2.36	3.23	4.42	4.47	4.64	4.40	2.62	3.35
FeO	13.77	7.93	7.27	7.27	6.83	6.25	5.62	6.20	6.16	6.89	7.39
MnO	0.26	0.11	0.17	0.20	0.14	0.20	0.17	0.17	0.18	0.14	0.17
MgO	7.36	12.16	11.08	7.94	8.25	7.64	8.40	6.88	6.79	9.54	6.28
CaO	8.89	9.82	12.30	15.38	12.24	12.65	13.18	11.67	12.47	11.62	11.30
Na_2O	1.97	2.88	2.22	2.06	2.90	2.91	2.94	3.42	3.32	3.12	4.23
K_2O	0.26	0.09	0.44	0.10	0.27	0.31	0.31	0.40	0.34	0.20	0.70
P_2O_5	0.16	0.13	0.10	0.14	0.15	0.08	0.09	0.17	0.16	0.07	0.20
CO_2	0.11	0.10	0.36	0.25	0.19	0.51	0.05	0.22	0.29	0.11	0.61
H_2O^+	1.31	0.83	1.15	0.93	1.87	1.50	1.22	1.67	1.51	1.72	1.11
H_2O^-	0.11	0.22	0.19	0.25	0.21	0.18	0.08	0.24	0.23	0.30	0.22
total	99.56	98.64	98.80	98.61	99.99	99.79	99.66	100.03	99.70	99.49	99.81

Microchemistry (ppm)

Cr	239	766	831	788	547	441	555	468	394	451	369
Sc	53.9	34.1	38.0	40.6	38.3	43.0	41.6	44.2	43.2	41.1	44.3
Ni	n.d.	319	301	240	206	114	161	230	204	191	164
Ba	85	16	7.9	10	44	28	12	30	32	35	90
Rb	13.2	<1	55	<1	<1	<1	<1	2.3	<1	<1	6.8
Sr	93	56	181	269	204	202	472	193	214	226	214
Th	n.d.	n.d.	n.d.	n.d.	n.d.	n.d.	n.d.	n.d.	n.d.	n.d.	1.26
Hf	2.5	1.70	1.42	1.64	3.39	1.70	2.02	2.82	3.09	1.65	2.86
Ta	n.d.	n.d.	n.d.	n.d.	n.d.	n.d.	n.d.	n.d.	n.d.	0.64	<1

REE concentrations (ppm)

La	2.8	1.5	1.2	2.0	4.9	2.5	3.0	6.0	6.0	2.3	5.6
Ce	8.0	5.1	4.2	7.3	15.4	7.6	8.9	16.2	15.1	6.5	16.4
Nd	8.5	11.0	6.0	11.4	n.d.	n.d.	n.d.	18.0	n.d.	n.d.	n.d.
Sm	3.06	1.56	1.65	2.37	4.02	2.37	2.60	3.93	3.63	2.12	3.86
Eu	1.22	0.66	0.74	1.00	1.49	0.90	1.03	1.36	1.34	0.89	1.44
Gd	5.32	3.37	2.29	2.64	n.d.	2.74	n.d.	5.93	n.d.	n.d.	n.d.
Tb	<1	<1	<1	<1	<1	<1	<1	<1	<1	0.48	<1
Tm	n.d.	0.33	0.37	n.d.	n.d.	n.d.	0.42	0.48	0.27	n.d.	n.d.
Ho	n.d.	n.d.	n.d.	n.d.	n.d.	n.d.	n.d.	n.d.	n.d.	n.d.	n.d.
Yb	3.15	1.40	1.89	2.50	0.46	2.40	2.24	2.97	3.01	2.16	3.16
Lu	0.54	0.25	0.38	0.38	0.52	0.54	0.41	0.47	0.44	0.45	0.48
Σ REE	32.59	25.17	18.6	29.59	26.59	19.0	18.6	55.34	29.73	14.90	30.94
$(Ce/Yb)_N$	0.51	0.73	0.45	0.59	6.77	0.64	0.80	1.10	1.01	0.60	1.06
$(Ce/Sm)_N$	0.55	0.69	0.54	0.65	0.81	0.68	0.73	0.87	0.88	0.65	0.90
Eu/Eu^*	1.03	0.97	1.30	1.34	(1.01)	1.19	(0.85)	0.96	(0.96)	(1.20)	(0.90)

Table 3
Selected analyses of various mafic rocks from different units (wt %)

	the Rataje Micaschist Zone									
	banded amphibolites									
	KH-1	KH-2	KH-8	KH-9	KH-10	KH-11	KH-6	KH-13	KH-29	KH-30
SiO_2	46.77	44.65	44.36	43.51	43.41	41.32	51.57	46.84	47.12	46.90
TiO_2	0.87	0.86	1.12	1.16	0.98	0.79	1.50	2.48	1.13	3.03
Al_2O_3	16.33	15.92	14.21	14.60	15.34	14.89	15.44	15.59	16.92	14.66
Fe_2O_3	2.12	2.31	3.50	3.62	1.72	1.00	2.12	4.43	2.86	2.55
FeO	7.49	6.69	6.25	6.64	7.34	6.69	8.07	6.93	7.07	8.22
MnO	0.14	0.15	0.18	0.15	0.14	0.16	0.14	0.18	0.12	0.17
MgO	8.72	7.74	5.89	4.45	5.23	8.64	4.45	5.13	7.74	7.28
CaO	11.12	13.77	13.59	15.15	15.01	17.26	9.08	10.85	10.51	10.80
Na_2O	3.16	3.20	4.55	3.43	3.34	2.69	3.90	3.81	3.68	2.71
K_2O	0.56	0.57	1.05	1.11	0.66	0.83	0.48	1.06	0.86	1.00
P_2O_5	0.07	0.08	0.15	0.14	0.11	0.10	0.17	0.45	0.21	0.95
CO_2	0.16	2.09	1.75	3.94	3.71	3.17	0.20	0.22	0.14	0.09
H_2O^+	1.72	1.46	0.85	0.95	0.84	1.20	1.04	1.26	1.58	1.35
H_2O^-	0.30	0.21	0.23	0.19	0.38	0.21	0.43	0.33	0.24	0.17
total	99.53	99.70	97.68	99.04	97.37	98.95	98.59	99.56	99.68	99.88

Microchemistry (ppm)

Cr	385	702	415	351	366	873	245	168	84	–
Sc	42.6	39.1	38.9	40.0	45.6	39.6	41.5	37.3	39.4	–
Ni	206	332	172	128	138	413	n.d.	73	n.d.	–
Ba	48	19	110	112	64	115	105	133	127	115
Rb	13.4	6.8	11.3	15.8	6.7	14.7	4.5	9.0	11.3	36.7
Sr	167	259	237	237	190	248	235	317	316	477
Th	n.d.	0.33	n.d.	n.d.	1.12	n.d.	2.93	1.87	4.12	–
Hf	1.68	1.49	1.87	1.93	1.44	1.24	4.28	5.09	5.35	–
Ta	0.17	n.d.	<1	<1	<1	n.d.	<1	1.6	3.02	–

REE concentrations (ppm)

La	2.1	2.7	3.5	3.7	3.0	2.6	15.2	19.9	32.2	–
Ce	7.2	8.1	9.4	10.7	10.0	7.7	34.8	44.1	64.2	–
Nd	4.4	n.d.	n.d.	n.d.	n.d.	n.d.	19.7	22.7	34.7	–
Sm	2.02	1.93	2.47	2.56	2.40	1.90	4.84	6.01	7.05	–
Eu	0.85	0.79	0.98	0.95	0.91	0.79	1.51	1.95	2.31	–
Gd	n.d.	n.d.	n.d.	n.d.	n.d.	3.67	n.d.	9.35	6.00	–
Tb	0.57	0.45	<1	<1	<1	<1	<1	<1	1.1	–
Tm	n.d.	n.d.	n.d.	0.39	n.d.	0.33	1.17	1.13	0.37	–
Yb	2.07	2.07	2.23	2.21	2.30	2.31	3.19	2.71	3.95	–
Lu	0.33	0.34	0.37	0.35	0.38	0.37	0.46	0.49	0.69	–
Σ REE	19.54	16.38	18.95	20.86	18.18	19.67	80.87	108.34	152.57	–
$(Ce/Yb)_N$	0.72	0.79	0.98	0.94	0.67	1.04	2.21	1.10	3.28	–
$(Ce/Sm)_N$	0.76	0.89	0.89	0.88	0.86	0.90	1.52	0.87	1.93	–
Eu/Eu^*	1.08	1.16	(1.0)	(1.0)	1.01	(1.0)	(0.7)	0.96	1.16	–

Appendix 3
Chemical composition of the rock-forming minerals

Table 1
Pyroxenes, selected analyses (wt %)

	Retrograded eclogite			Massive amphibolite				Metagabbro				Banded amphibolite
	KH-34: Poličany			KH-22: Mančice				Moravany		Svatý Kříž		Chedrbí
	core	rim	rim	core	rim	core	rim	opx	cpx	cpx	cpx	cpx
SiO_2	52.03	53.57	53.92	50.86	49.65	50.76	49.79	50.71	51.37	53.00	52.96	50.47
TiO_2	0.12	0.63	0.53	0.56	0.58	0.51	0.53	0.10	0.12	0.15	–	0.32
Al_2O_3	1.68	5.08	4.42	8.35	8.58	9.27	9.10	1.35	2.13	1.87	1.77	2.73
FeO_{tot}	10.42	11.40	10.90	12.26	12.35	11.77	12.41	19.77	7.21	6.21	6.33	9.76
MnO	0.35	0.20	0.17	0.19	0.16	0.18	0.17	0.54	0.25	0.23	0.22	0.30
MgO	12.08	16.19	17.23	14.89	15.49	15.39	15.47	24.25	16.40	15.68	14.64	10.67
CaO	22.75	11.70	11.73	10.86	11.14	11.21	11.14	0.51	21.79	21.67	22.90	24.83
Na_2O	0.53	1.20	1.08	1.92	2.01	1.94	1.94	0.03	0.36	0.36	0.36	0.90
K_2O	0.03	0.02	0.01	0.05	0.09	0.05	0.02	–	–	0.01	–	–
total	99.96	99.99	99.99	99.94	100.01	101.12	100.60	97.27	99.63	99.16	99.19	99.98
Si	1.962	1.952	1.960	1.867	1.830	1.840	1.823	1.929	1.913	1.965	1.971	1.916
Al	0.038	0.048	0.040	0.133	0.170	0.160	0.177	0.060	0.087	0.035	0.029	0.084
Al	0.037	0.170	0.149	0.228	0.202	0.235	0.215	–	0.006	0.046	0.048	0.099
Ti	0.003	0.017	0.014	0.015	0.016	0.014	0.015	0.003	0.003	0.004	–	0.018
Fe^{3+}*	0.000	0.000	0.000	0.014	0.080	0.033	0.072	0.079	0.100	0.006	0.006	0.000
Fe^{2+}	0.328	0.347	0.331	0.362	0.301	0.324	0.308	0.549	0.124	0.186	0.190	0.310
Mn	0.011	0.006	0.005	0.006	0.005	0.006	0.005	0.017	0.007	0.007	0.007	0.010
Mg	0.678	0.880	0.934	0.815	0.851	0.831	0.844	1.375	0.910	0.848	0.811	0.604
Ca	0.919	0.457	0.457	0.427	0.440	0.435	0.437	0.020	0.869	0.860	0.913	1.009
Na	0.039	0.085	0.076	0.137	0.144	0.136	0.138	0.002	0.025	0.025	0.025	0.033
K	0.001	0.001	–	0.002	0.002	0.004	0.002	0.001	–	–	–	–

End-members (mol. %)

En	33.70	45.24	47.85	40.97	40.06	41.55	41.80	67.33	44.58	42.87	40.55	29.25
Fs	16.85	18.15	17.21	19.20	19.08	18.15	19.07	31.59	11.31	10.06	10.15	15.50
Wo	45.67	23.50	23.41	21.47	21.75	21.75	21.64	0.98	42.57	43.48	45.65	48.86
Eg	1.94	4.37	3.89	6.89	7.12	6.80	6.83	0.10	1.22	1.26	1.25	1.60
Ts	1.84	8.74	7.63	11.46	9.98	11.75	10.65	–	0.29	2.32	2.40	4.79

200 Wo/Wo + Fs + En

	94.96	54.09	52.92	52.60	53.48	53.40	52.97	1.96	86.47	90.20	94.76	104.39

100 Fs/Fs + En

	33.33	28.63	26.45	34.38	31.20	30.40	31.33	31.93	20.24	19.00	20.02	34.64

*Fe^{3+} calculated as 4 -2Si -2Ti -Al +(Na+K) according to Ryburn et al. (1976)

Table 2a
Amphiboles, selected analyses (wt %)

	Retrograded eclogite					Least retrograded eclogite				Retrograded eclogite					
	KH-34					KH-32				KH-25		KH-21		KH-23	
	core	core	rim	core	rim	core	rim	core	rim	core	rim	core	rim	core	rim
SiO_2	39.93	43.11	43.13	44.44	45.20	41.09	41.94	42.63	42.80	38.58	38.86	43.91	46.23	41.17	41.23
TiO_2	0.52	0.52	0.52	0.85	0.80	0.65	0.69	0.52	0.44	0.90	0.79	0.76	0.84	1.32	1.35
Al_2O_3	16.46	14.27	14.31	10.75	10.49	14.14	13.82	12.23	12.20	15.43	16.69	11.13	8.65	13.00	11.23
FeO^{tot}	15.76	15.65	15.71	16.57	16.20	10.88	10.53	10.76	10.74	15.62	13.87	18.57	19.19	15.11	15.39
MnO	0.19	0.26	0.24	0.30	0.32	0.21	0.20	0.28	0.29	0.15	0.08	0.20	0.12	0.04	0.10
MgO	9.99	11.24	11.06	10.62	10.42	13.99	13.73	14.95	14.70	11.50	11.07	9.93	9.80	11.44	11.34
CaO	10.91	8.16	8.36	11.63	11.84	13.82	13.72	13.82	13.89	12.98	13.07	10.10	10.39	12.89	12.90
Na_2O	3.16	3.61	3.47	1.40	1.30	1.59	1.48	1.41	1.47	2.38	2.47	2.27	1.68	1.91	2.25
K_2O	0.03	0.14	0.07	0.40	0.39	0.88	0.83	0.84	0.69	0.07	0.05	0.09	0.08	0.11	0.06
total	96.95	96.96	96.87	96.96	96.96	97.25	96.94	97.44	97.22	97.61	96.95	96.96	96.98	96.99	95.85
Si	6.013	6.412	6.419	6.673	6.764	6.089	6.205	6.289	6.322	5.823	5.841	6.635	6.968	6.199	6.312
Al	1.987	1.588	1.581	1.327	1.236	1.911	1.795	1.711	1.678	2.177	1.159	1.365	1.032	1.801	1.688
Al	0.934	0.914	0.929	0.575	0.614	0.559	0.615	0.416	0.445	0.568	0.798	0.617	0.505	0.505	0.338
Ti	0.059	0.058	0.058	0.096	0.090	0.072	0.077	0.058	0.049	0.102	0.089	0.086	0.095	0.149	0.155
Fe	1.765	1.535	1.559	1.952	1.971	1.278	1.280	1.238	1.269	1.742	1.632	2.060	2.198	2.568	2.588
Mg	2.242	2.492	2.454	2.377	2.325	3.091	3.028	3.288	3.237	2.588	2.481	2.237	2.202	1.778	1.919
Fe	0.220	0.411	0.397	0.129	0.056	0.071	0.023	0.089	0.058	0.229	0.111	0.286	0.222	0.125	0.051
Mn	0.024	0.033	0.030	0.038	0.041	0.026	0.025	0.035	0.036	0.019	0.010	0.026	0.015	0.005	0.013
Ca	1.756	1.300	1.333	1.833	1.898	1.903	1.952	1.876	1.906	1.752	1.878	1.635	1.678	1.870	1.036
Na	–	0.255	0.240	–	0.005	–	–	–	–	–	–	0.053	0.085	–	–
Ca	0.004	–	–	0.038	–	0.292	0.223	0.309	0.292	0.347	0.226	–	–	0.209	0.180
Na	0.923	0.786	0.762	0.408	0.372	0.457	0.425	0.403	0.421	0.696	0.720	0.612	0.406	0.558	0.668
K	0.006	0.027	0.013	0.077	0.074	0.166	0.157	0.158	0.130	0.013	0.010	0.017	0.015	0.021	0.012
Mg/Mg+Fe	0.53	0.56	0.56	0.53	0.53	0.70	0.70	0.71	0.71	0.57	0.59	0.49	0.48	0.57	0.57
variety	Prg	Prg-Hbl		Hbl		Prg		Prg-Hbl		Prg			Hbl	Prg-Hbl	

Table 2b
Amphiboles, selected analyses (wt %)

	Banded amphibolite				striped amphibolite				banded amphibolite		banded amphibolite	
	KH-8 Chedrbí				KH-19 Kbílek				KH-15 Markovice		KH-6 Třebonín	
	core	core	rim	core	core	rim	core	rim	core	rim	core	rim
SiO_2	38.14	37.99	39.24	38.80	40.10	40.72	44.21	44.26	44.21	43.17	43.10	45.45
TiO_2	1.64	1.33	1.54	1.47	1.06	1.15	0.89	0.78	0.89	0.86	1.15	1.11
Al_2O_3	12.26	12.09	12.34	12.40	13.17	13.82	11.11	11.83	11.11	11.35	11.28	10.55
FeO^{tot}	17.14	17.17	16.94	17.33	10.31	10.48	17.52	17.08	17.52	18.69	18.39	17.25
MnO	0.27	0.35	0.26	0.32	0.23	0.20	0.14	0.14	0.14	0.31	0.27	0.28
MgO	8.95	8.30	9.01	8.51	14.05	13.11	10.41	10.46	10.41	9.36	9.65	10.14
CaO	13.89	13.89	14.32	14.43	14.53	14.29	10.29	9.98	10.29	11.34	11.28	11.42
Na_2O	2.13	2.24	1.89	1.92	2.34	1.93	2.30	2.37	2.30	1.49	1.61	1.18
K_2O	1.32	1.77	1.54	1.75	0.68	0.77	0.08	0.08	0.08	0.41	0.44	0.36
total	95.74	96.73	98.73	98.57	98.19	98.20	96.95	96.98	96.95	96.98	97.17	97.74
Si	7.000	7.099	7.112	7.100	6.979	7.074	6.646	6.626	6.646	6.558	6.531	6.761
Al	1.000	0.901	0.888	0.900	1.021	0.926	1.354	1.374	1.354	1.442	1.469	1.239
Al	1.652	1.762	1.748	1.774	1.681	1.903	0.615	0.713	0.615	0.590	0.545	0.611
Ti	0.226	0.187	0.210	0.202	0.139	0.150	0.101	0.088	0.101	0.098	0.131	0.124
Mg	2.449	2.312	2.434	2.322	3.180	2.947	2.333	2.334	2.333	2.120	2.180	2.249
Fe	0.673	0.739	0.608	0.702	–	–	1.952	1.860	1.952	2.192	2.144	2.016
Mg	–	–	–	–	0.465	0.448	–	–	–	–	–	–
Fe	1.958	1.945	1.960	1.950	1.501	1.522	0.251	0.273	0.251	0.183	0.186	0.130
Mn	0.042	0.055	0.040	0.050	0.034	0.029	0.018	0.010	0.018	0.040	0.035	0.035
Ca	2.731	2.781	2.781	2.829	2.710	2.660	1.657	1.601	1.657	1.777	1.779	1.820
Na	–	–	–	–	–	–	0.074	0.109	0.074	–	–	0.015
Ca	–	–	–	–	–	–	–	–	–	0.068	0.052	–
Na	0.758	0.812	0.664	0.681	0.790	0.650	0.596	0.579	0.596	0.439	0.473	0.326
K	0.309	0.422	0.356	0.409	0.151	0.171	0.015	0.010	0.015	0.079	0.085	0.068
Mg/Mg+Fe=	0.48	0.46	0.49	0.47	0.71	0.69	0.51	0.59	0.51	0.47	0.48	0.51
variety	Al-Fe-Eden				Al-Ed		Ed-Hbl					Mg-Hbl

Table 2c

Amphiboles, selected analyses (wt %)

	Massive amphibolite					Massive amphibolite				Amphibolite	Garnet amphibolite		
	KH-3, Český Šternberk			KH-22, Mančice		KH-31, Víska				Ronov[1]	KH-35, Žehušice		
	core	core	rim	core	rim	core	rim	core	rim	core	core	rim	rim
SiO_2(%)	44.13	44.67	45.39	46.82	48.20	43.64	42.60	44.60	44.36	41.51	42.24	41.80	41.78
TiO_2	1.08	1.05	0.96	0.58	0.50	1.01	1.23	0.66	0.68	1.12	1.22	1.15	1.11
Al_2O_3	11.26	11.55	10.94	10.18	9.67	13.48	12.85	12.68	12.55	12.50	13.35	13.53	13.53
FeO^{tot}	17.57	17.26	16.89	12.12	12.12	13.71	13.44	13.92	13.88	20.24	14.33	14.42	14.00
MnO	0.29	0.24	0.27	0.19	0.12	0.20	0.16	0.26	0.20	0.21	0.21	0.19	0.24
MgO	9.50	9.57	9.30	14.21	13.67	12.73	12.70	13.20	13.14	7.64	11.34	11.15	11.33
CaO	11.49	11.16	11.76	10.69	10.71	10.46	10.66	10.49	10.37	10.41	13.58	12.98	13.55
Na_2O	1.77	1.63	1.60	2.10	1.93	2.96	2.97	2.69	2.81	1.20	1.75	1.64	1.62
K_2O	0.33	0.32	0.32	0.08	0.05	0.27	0.27	0.22	0.24	0.84	0.11	0.11	0.12
total	97.42	97.45	97.43	96.97	96.97	98.46	96.88	98.72	98.23	95.66	98.13	96.97	97.28
Si	6.628	6.672	6.773	6.836	7.006	6.373	6.340	6.487	6.487	6.444	6.256	6.257	6.235
Al	1.372	1.328	1.227	1.164	0.994	1.627	1.660	1.513	1.513	1.556	1.744	1.743	1.765
Al	0.622	0.705	0.697	0.588	0.662	0.693	0.594	0.660	0.650	0.732	0.586	0.644	0.615
Ti	0.122	0.118	0.108	0.064	0.055	0.111	0.138	0.072	0.075	0.131	0.136	0.129	0.125
Mg	2.127	2.131	2.069	3.093	2.962	2.771	2.818	2.862	2.865	1.766	2.504	2.488	2.521
Fe	2.129	2.046	2.108	1.256	1.321	1.424	1.451	1.405	1.411	2.371	1.774	1.739	1.740
Mn	–	–	0.019	–	–	–	–	–	–	–	–	–	–
Fe	0.078	0.110	–	0.224	0.152	0.025	0.222	0.288	0.287	0.257	–	0.066	0.008
Mn	0.037	0.030	0.015	0.023	0.015	0.025	0.020	0.032	0.025	0.027	0.026	0.024	0.030
Na	0.036	0.073	0.105	0.080	0.165	0.088	0.058	0.046	0.064	–	–	–	–
Ca	1.849	1.786	1.880	1.672	1.668	1.637	1.700	1.635	1.624	1.716	1.973	1.910	1.962
Ca	–	–	–	–	–	–	–	–	–	0.015	0.182	0.172	0.205
Na	0.479	0.399	0.358	0.514	0.379	0.750	0.798	0.713	0.733	0.351	0.503	0.476	0.469
K	0.063	0.061	0.061	0.015	0.009	0.050	0.051	0.041	0.045	0.167	0.021	0.021	0.023
Mg/Mg+Fe	0.49	0.50	0.49	0.67	0.67	0.62	0.63	0.63	0.63	0.40	0.58	0.50	0.59
variety	Ed-Hbl		Fe-Hbl	Ed	Hbl	Prg-Hbl					Ts-Hbl		

Table 2d
Amphiboles, selected analyses (wt %)

	banded amphibolite			banded amphibolite		banded amphibolite		
	KH-17, Malešov			KH-13, Okřesaneč		KH-29, Hodkov		
	core	rim	rim	core	rim	core	rim	rim
SiO_2(%)	44.25	45.33	45.25	40.55	40.52	43.29	43.20	44.66
TiO_2	0.64	0.83	0.45	1.33	1.40	1.11	1.06	1.01
Al_2O_3	13.30	11.66	11.51	10.84	11.14	11.80	12.28	11.71
FeO^{tot}	14.60	15.78	14.15	21.80	22.26	15.20	14.87	14.42
MnO	0.30	0.29	0.22	0.45	0.26	0.27	0.27	0.34
MgO	11.37	11.35	11.96	7.78	7.53	11.40	11.06	11.50
CaO	11.72	11.97	11.93	11.50	11.34	11.58	11.95	11.59
Na_2O	1.88	1.69	1.49	2.01	1.80	2.40	2.36	2.07
K_2O	0.45	0.42	0.27	1.22	1.22	0.43	0.42	0.39
total	98.51	99.32	97.23	97.48	97.47	97.48	97.47	97.69
Si	6.480	6.615	6.681	6.322	6.315	6.463	6.443	6.597
Al	1.520	1.385	1.319	1.678	1.685	1.537	1.557	1.403
Al	0.776	0.620	0.684	0.314	0.361	0.539	0.601	0.636
Ti	0.070	0.091	0.050	0.156	0.164	0.125	0.119	0.112
Mg	2.482	2.469	2.633	1.808	1.750	2.537	2.459	2.532
Fe	1.672	1.820	1.633	2.722	2.725	1.799	1.821	1.720
Fe	0.117	0.106	0.114	0.121	0.176	0.099	0.034	0.062
Mn	0.037	0.036	0.028	0.059	0.034	0.034	0.034	0.043
Ca	1.839	1.858	1.859	1.820	1.789	1.852	1.910	1.834
Na	0.007	–	–	–	–	0.014	0.022	0.062
Ca	–	0.013	0.029	0.101	0.104	–	–	–
Na	0.526	0.478	0.427	0.608	0.544	0.680	0.660	0.531
K	0.084	0.078	0.051	0.243	0.243	0.082	0.080	0.073
Mg/Mg+Fe	0.58	0.56	0.60	0.39	0.38	0.57	0.57	0.59
variety	Prg-Hbl		Mg-Hbl	Prg-Hbl		Prg-Hbl		Ed-Hbl

Table 3a

Garnets, selected analyses (wt %)

	Retrograded eclogite								Retrograded eclogite				
	KH-34, Poličany	KH-32, Poličany		KH-25, Libodřice					KH-21, Mančice		KH-23, Mančice		
	core	core	rim	core	rim	core	transit.	rim	core	rim	core	transit.	rim
SiO_2	39.94	26.50	28.79	38.36	39.11	38.12	38.48	38.49	38.27	38.85	35.97	35.49	36.48
TiO_2	0.11	–	0.03	0.19	0.29	0.24	0.23	0.19	0.14	0.11	0.44	0.32	0.15
Cr_2O_3	n.d.	n.d.	n.d.	n.d.	n.d.	0.04	0.12	0.11	n.d.	n.d.	–	0.42	0.61
Al_2O_3	19.94	22.48	14.98	21.93	21.50	23.03	23.29	23.68	20.29	20.04	21.95	22.30	22.40
FeO^{tot}	24.05	20.29	18.93	23.40	22.14	24.21	23.61	23.34	25.79	25.40	24.12	25.18	23.15
MnO	0.64	0.29	0.25	2.94	4.20	3.83	4.23	2.45	1.18	1.56	3.69	2.87	0.36
MgO	6.59	19.68	19.56	1.85	1.03	1.51	1.27	1.57	1.64	1.70	1.34	1.30	3.19
CaO	8.70	10.72	17.40	11.22	11.66	8.83	8.64	10.10	12.66	12.29	12.38	12.00	13.58
total	99.97	99.96	99.94	99.89	99.93	99.81	99.87	99.93	99.97	99.95	99.89	99.88	99.92
Si	6.180	4.218	4.670	6.032	6.144	5.997	6.032	5.998	6.075	6.152	5.757	5.691	5.742
Al	–	1.782	1.330	–	–	0.003	–	0.002	–	–	0.243	0.309	0.258
Al	3.637	2.435	1.534	4.065	3.981	4.300	4.303	4.347	3.796	3.740	3.897	3.906	3.897
Ti	0.013	–	0.003	0.022	0.034	0.028	0.027	0.022	0.017	0.013	0.053	0.039	0.018
Cr	–	–	–	–	–	0.005	0.015	0.014	–	–	–	0.053	0.076
Fe	3.112	2.701	2.568	3.077	2.909	3.185	3.095	3.042	3.424	3.364	3.228	3.377	3.047
Mn	0.084	0.039	0.034	0.392	0.559	0.510	0.562	0.323	0.159	0.209	0.500	0.390	0.048
Mg	1.520	4.670	4.730	0.434	0.241	0.354	0.297	0.365	0.388	0.401	0.320	0.311	0.749
Ca	1.442	1.828	3.024	1.890	1.963	1.488	1.451	1.686	2.153	2.085	2.123	2.062	2.290
Sum	15.988	15.891	15.563	15.922	15.831	15.870	15.782	15.799	16.012	15.964	16.121	16.138	16.125

End-members (mol. %)

Alm	50.48	29.23	24.80	53.02	51.13	57.37	57.12	56.04	55.83	55.45	52.04	54.83	49.61
Spess	1.36	0.41	0.33	6.75	9.82	9.19	10.37	5.96	2.58	3.46	8.07	6.33	0.78
Pyr	24.66	50.56	45.67	7.47	4.24	6.37	5.48	6.72	6.33	6.62	5.16	5.04	12.18
Gross	23.19	19.79	29.20	32.18	33.90	26.16	25.87	30.29	34.84	34.16	33.40	31.55	35.14
Ti-Gross	0.31	–	–	0.58	0.90	0.76	0.75	0.61	0.41	0.32	1.28	0.94	0.43
Uvar	–	–	–	–	–	0.13	0.41	0.31	–	–	–	1.30	1.85

Table 3b
Garnets, selected analyses (wt %)

	Garnetiferous amphibolite				Amphibolite + Gt		Migmatized amphibolite			Gt amphibolite	
	Pl-69 I, Plaňany		Pl-76, Plaňany		Pl-66, Plaňany		Ronov			KH-35, Žehušice	
	core	rim	core	rim	core	rim	core	trans.	rim	core	rim
SiO_2(%)	38.04	38.00	37.59	37.47	37.92	37.74	38.21	37.91	37.75	42.24	43.64
TiO_2	0.08	0.78	0.22	0.40	0.05	0.05	0.12	0.03	0.21	1.23	1.10
Cr_2O_3	n.d.	n.d.	n.d.	n.d.	n.d.	n.d	n.d.	n.d.	n.d.	0.00	0.00
Al_2O_3	20.78	20.84	21.51	21.49	22.18	22.04	21.46	21.61	21.63	14.19	13.99
FeO*	27.00	26.35	28.82	28.20	22.94	22.24	25.49	25.40	25.20	15.53	15.57
MnO	0.62	0.47	0.76	1.03	0.82	1.19	0.86	0.83	1.03	0.26	0.23
MgO	2.78	3.13	4.12	3.71	3.88	3.58	2.99	3.21	2.97	11.11	10.75
CaO	9.71	9.83	7.52	8.48	11.26	12.18	11.40	10.89	11.46	13.82	13.01
Na_2O	–	–	–	–	–	–	0.06	0.05	0.06	–	–
total	99.00	99.40	100.54	100.78	99.05	99.02	100.59	99.92	100.31	98.38	98.29
Si	6.067	6.017	5.920	5.898	5.958	5.943	5.980	5.964	5.930	6.499	6.678
Al	–	–	0.080	0.102	0.042	0.057	0.020	0.036	0.070	–	–
Al	3.900	3.884	3.906	3.876	4.057	4.024	3.940	3.972	3.791	2.573	2.523
Ti	0.009	0.092	0.026	0.050	0.006	0.006	0.014	0.004	0.024	0.142	0.127
Fe	3.588	3.480	3.782	3.696	3.003	2.918	3.336	3.343	3.309	1.998	1.992
Mn	0.082	0.062	0.102	0.137	0.109	0.158	0.115	0.110	0.136	0.034	0.030
Mg	0.665	0.743	0.974	0.876	0.915	0.847	0.698	0.751	0.696	2.548	2.452
Ca	1.660	1.668	1.270	1.431	1.896	2.055	1.912	1.836	1.929	2.278	2.133
Na	–	–	–	–	–	–	0.016	0.014	0.016	–	–
Sum	15.971	15.946	16.060	16.066	15.986	16.008	16.031	16.030	15.901	16.072	15.935

End-members (mol. %)

Alm	59.8	58.5	61.7	60.2	50.7	48.8	55.0	55.4	54.4	28.83	29.87
Spess	1.4	1.0	1.7	2.2	1.8	2.6	2.0	1.8	2.4	0.49	0.45
Pyr	11.1	12.5	15.9	14.3	15.5	14.2	11.5	12.5	11.5	36.77	36.76
Gross	27.7	28.0	20.7	23.3	32.0	34.4	31.5	30.3	31.7	30.82	30.07
Ti-Gross	–	–	–	–	–	–	–	–	–	3.08	2.85

Table 4a

Plagioclases, selected analyses (wt %)

	Retrograded eclogite				Retrograded eclogite			Massive amphibolite				Gt. amphibolite	
	KH-34, Poličany		KH-32, Poličany		KH-21, Mančice		KH-23	KH-3, Č. Šternberk		KH-31, Víska		KH-4, Kácov	
	core	rim	core	rim	core	core	core	core	rim	core	rim	core	core
SiO_2	67.15	67.82	57.24	56.33	65.91	66.46	63.04	59.36	58.79	63.84	62.82	60.90	59.49
TiO_2	0.05	0.01	–	–	0.03	0.01	0.04	0.01	–	–	0.01	–	0.02
Al_2O_3	20.79	20.44	25.15	25.37	21.28	20.91	23.58	25.78	26.14	21.86	22.58	22.60	23.90
FeO^{tot}	0.19	2.22	0.37	0.19	0.25	0.38	0.32	0.11	0.25	0.16	0.15	0.04	0.08
MnO	0.03	–	0.06	0.06	–	–	–	0.03	0.04	–	–	–	0.07
MgO	–	–	0.75	–	0.01	–	–	–	0.01	–	–	–	–
CaO	2.32	1.52	7.48	8.30	2.76	2.13	3.65	6.93	7.28	3.64	4.67	8.02	8.66
Na_2O	9.46	10.04	8.58	7.74	9.67	10.03	9.33	7.72	7.43	9.10	8.40	8.27	7.59
K_2O	–	–	0.18	0.16	0.09	0.07	0.02	0.05	0.05	0.01	0.01	0.17	0.19
total	99.99	102.05	99.81	98.15	100.00	99.99	99.98	99.99	99.99	98.61	98.64	100.00	100.00
Si	11.744	11.731	10.356	10.347	11.582	11.668	11.136	10.590	10.505	11.401	11.240	10.917	10.686
Al	4.285	4.167	5.363	5.492	4.407	4.327	4.909	5.421	5.505	4.601	4.761	4.775	5.060
Ti	0.007	0.001	–	–	0.004	0.001	0.005	0.001	–	–	0.001	–	0.003
T=	16.036	15.899	15.719	15.839	15.994	15.996	16.050	16.012	16.010	16.002	16.002	15.692	15.749
Fe	0.028	0.321	0.056	0.029	0.037	0.056	0.043	0.016	0.037	0.024	0.022	0.006	0.012
Mn	0.004	–	0.009	0.009	–	–	–	0.005	0.006	–	–	–	0.011
Mg	–	–	0.202	–	0.003	–	–	–	0.003	–	–	–	–
Ca	0.435	0.282	1.450	1.633	0.520	0.401	0.691	1.325	1.394	0.696	0.895	1.540	1.667
Na	3.208	3.367	3.010	2.756	3.295	3.414	3.195	2.670	2.574	3.151	2.914	2.874	2.643
K	–	–	0.042	0.037	0.020	0.016	0.005	0.011	0.011	0.002	0.002	0.039	0.044

Mol. %

An	11.93	7.72	32.21	36.89	13.55	10.46	17.75	33.06	35.02	18.09	23.49	34.59	38.28
Ab	88.07	92.28	66.86	62.26	85.92	89.13	82.13	66.05	64.69	81.85	76.45	64.54	60.72
Or	–	–	0.92	0.85	0.53	0.41	0.12	0.28	0.29	0.05	0.06	0.87	1.00

*Total iron assumming as Fe_2O_3

Table 4b
Plagioclases and K-feldspar, selected analyses (wt %)

	striped amphibolite			banded amphibolite				banded amphibolite		
	KH-19, Kbílek			KH-8, Chedrbí		KH-6, Třebonín		KH-15, Markovice		KH-17, Malešov
	core	core	rim	core	rim	core	rim	core	core	core
SiO_2	62.32	47.84	64.31	56.51	59.59	58.12	59.08	54.34	59.93	60.98
TiO_2	0.09	0.03	0.06	-	0.09	0.01	0.01	0.08	-	-
Al_2O_3	23.48	30.97	18.10	25.83	24.58	25.26	24.57	28.80	24.08	23.66
FeO^{tot}	0.10	-	0.18	-	0.31	0.08	0.08	0.55	0.19	0.08
MnO	0.02	0.07	0.02	0.26	0.05	-	-	0.02	-	-
MgO	-	-	-	0.03	0.01	0.01	-	0.10	0.02	0.02
CaO	8.40	18.42	-	10.51	8.93	8.21	7.30	11.54	6.65	6.24
Na_2O	8.13	2.63	0.38	6.61	6.22	6.36	6.70	4.57	8.02	6.73
K_2O	0.21	0.03	17.30	0.24	0.22	0.12	0.08	0.08	0.11	0.08
total	100.94	99.99	100.35	100.00	100.00	98.17	97.82	99.99	99.00	97.79
Si	11.067	8.857	11.945	10.230	10.663	10.565	10.739	9.821	10.799	11.016
Al	4.535	6.758	3.962	5.511	5.184	5.412	5.264	6.135	5.114	5.037
Ti	0.012	0.004	0.008	-	0.012	0.001	0.001	0.011	-	-
T =	15.614	15.619	15.916	15.741	15.860	15.979	16.004	15.967	15.913	16.053
Fe	0.015	0.011	0.028	0.039	0.046	0.012	0.012	0.083	0.029	0.012
Mn	0.003	-	0.003	-	0.008	-	-	0.003	-	-
Mg	-	-	-	0.008	0.003	0.003	-	0.003	0.005	0.005
Ca	1.598	3.654	-	2.038	1.712	1.599	1.422	2.235	1.284	1.208
Na	2.799	0.944	0.137	2.320	2.158	2.242	2.361	1.601	2.802	2.357
K	0.048	0.007	4.099	0.055	0.050	0.028	0.019	0.018	0.025	0.018

Mol. %

An	35.95	79.34	-	46.18	43.67	41.33	37.40	57.97	31.23	33.70
Ab	62.97	20.50	3.23	52.56	55.05	57.95	62.11	41.55	68.16	65.78
Or	1.07	0.15	96.77	1.25	1.28	0.72	0.49	0.48	0.61	0.52

*Total iron assumming as Fe_2O_3

Table 4c
Plagioclases, selected analyses (wt %)

	banded amphibolite				pyrox. amphibolite	
	KH-13, Okřesaneč		KH-29, Hodkov		KH-22, Mančice	
	core	rim	core	rim	core	rim
SiO_2	59.36	61.69	59.81	61.48	66.29	67.09
TiO_2	–	0.04	0.02	–	0.03	-
Al_2O_3	23.18	22.53	25.61	23.09	20.27	19.87
FeO^{tot}	0.13	0.16	0.14	0.17	0.15	0.07
MnO	–	–	–	–	0.03	0.04
MgO	–	–	0.01	0.01	–	0.02
CaO	7.44	5.80	8.80	5.70	3.46	2.91
Na_2O	8.32	9.26	6.80	7.24	9.73	9.96
K_2O	0.15	0.19	0.04	0.03	0.02	0.03
total	98.58	99.67	101.23	97.72	99.98	99.99
Si	10.796	11.046	10.568	11.110	11.671	11.782
Al	4.969	4.754	5.333	4.918	4.206	4.112
Ti	–	0.005	0.003	–	0.004	–
T =	15.765	15.806	15.904	16.028	15.880	15.894
Fe	0.020	0.024	0.021	0.026	0.022	0.010
Mn	–	–	–	–	0.004	0.006
Mg	–	–	0.003	0.003	–	0.005
Ca	1.450	1.113	1.666	1.104	0.653	0.548
Na	2.934	3.215	2.330	2.537	3.321	3.391
K	0.035	0.043	0.009	0.007	0.004	0.007

Mol. %

An	32.81	25.45	41.60	30.26	16.40	13.88
Ab	66.40	73.55	58.17	69.55	83.48	85.95
Or	0.79	0.99	0.22	0.19	0.11	0.17

*Total iron assumming as Fe_2O_3

Table 5
Clinozoisite-epidote and prehnite, selected analyses (wt %)

	Striped amphibolite						Skarn	striped amphibolite	
	KH-19, Kbílek						Vlastějovice	KH-19, Kbílek	Markovice
	core	rim	core	rim	core	rim	Z-2S	prehnite	prehnite[1]
SiO_2	35.85	35.82	37.41	36.48	36.42	37.10	37.16	46.74	42.76
TiO_2	0.15	0.14	0.17	0.11	0.20	0.10	0.09	0.04	-
Al_2O_3	24.46	25.43	23.64	24.56	25.00	25.06	22.55	32.36	24.83
Fe_2O_3	9.14	8.37	11.17	9.42	9.47	9.31	13.62	-	0.13
FeO	1.13	0.55	0.10	0.87	1.64	0.74	0.70	0.21	1.12
MnO	0.08	0.05	0.13	0.16	0.17	0.19	0.10	-	0.05
MgO	-	-	-	-	-	-	0.10	-	0.07
CaO	24.44	25.01	24.43	24.25	24.68	24.37	22.78	14.84	26.84
Na_2O	-	-	0.01	0.01	-	-	0.21	1.85	0.03
K_2O	-	-	-	-	-	-	0.13	0.11	0.18
(H_2O^+)	2.82	2.75	3.08	2.87	2.90	2.88	1.89	4.56	4.24
F	-	-	-	-	-	-	0.028	-	-
H_2O^-	-	-	-	-	-	-	0.04	-	-
total	98.09	98.12	100.15	98.73	100.48	99.76	99.40	100.71	100.25
Si	3.003	2.977	3.083	3.030	2.987	3.040	2.992	6.096	5.896
Al	-	0.023	-	-	0.013	-	0.008	1.904	2.104
Z=	3.003	3.000	3.083	3.030	3.000	3.000	3.000	8.000	8.000
Al	2.414	2.468	2.296	2.404	2.403	2.420	2.132	3.070	1.931
Fe^{3+}	0.576	0.523	0.693	0.589	0.584	0.574	0.912	0.023	0.129
Ti	0.009	0.009	0.011	0.007	0.012	0.006	0.047	0.004	-
Fe^{2+}	0.079	0.038	0.007	0.061	0.112	0.051	0.012	-	0.013
Mn^{3+}	0.005	0.003	0.008	0.010	0.011	0.012	0.007	-	-
Y=	3.084	3.041	3.015	3.071	3.123	3.063	3.011	3.097	2.094
Mn^{2+}	0.001	0.001	0.001	0.001	0.001	0.001	0.007	-	0.006
Ca	2.193	2.227	2.157	2.158	2.169	2.139	1.965	2.074	3.965
Na	-	-	0.002	0.002	-	0.002	0.033	0.468	0.008
K	-	-	-	-	-	-	0.013	0.018	0.032
X=	2.194	2.228	2.160	2.161	2.170	2.142	2.018	2.560	4.005
OH	-	-	-	-	-	-	1.015	4.000	4.000
F	-	-	-	-	-	-	0.007	-	-
% Ps	19.2	17.5	23.2	19.7	19.5	19.2	30.0	0.74	6.26
% Al_2Fe^{3+}	56.6	56.7	57.7	57.2	56.4	57.5	60.5		

Note: Ps=100 $Fe^{3+}/Fe^{3}+$ + Al (pistacite), prehnite analysis from Kratochvíl (1934)

Table 6
Chlorites, selected analyses (wt %)

	Striped amphibolite		banded amphibolite			banded amphibolite			eclogite	amphibolite
	KH-19, Kbílek		KH-13, Okřesaneč		KH-29, Hodkov	KH-15, Markovice		KH-6, Třebonín	KH-34, Poličany	KH-31, Víska
	core	rim	core	rim	core	core	rim	core	core	core
SiO_2 (%)	26.31	26.20	33.09	28.97	29.34	27.93	27.34	27.93	27.31	30.49
TiO_2	0.07	0.05	0.06	0.15	0.08	0.06	0.08	0.10	0.07	0.21
Al_2O_3	19.48	19.29	17.05	20.15	18.66	19.56	18.66	19.29	18.86	17.54
FeO^{tot}	17.18	16.11	25.02	26.41	26.02	24.53	26.02	27.12	26.11	18.43
MnO	0.24	0.21	0.28	0.24	0.12	0.28	0.12	0.07	0.17	0.05
MgO	19.19	16.11	10.68	15.84	15.20	13.88	15.20	14.71	14.79	19.60
CaO	0.01	–	0.29	0.08	0.08	0.14	0.08	0.12	0.20	0.23
Na_2O	–	0.01	0.09	0.04	–	0.02	0.00	0.02	0.02	–
K_2O	0.01	0.01	0.29	0.03	0.03	0.03	0.03	0.03	0.03	0.12
total	82.49	77.99	86.85	91.91	89.53	86.43	87.53	89.39	87.56	86.67
Si	2.836	2.838	3.455	3.011	2.959	3.013	3.109	2.898	2.910	3.109
Al	1.174	1.162	0.545	0.989	1.041	0.987	0.891	1.102	1.090	0.891
T =	4.000	4.000	4.000	4.000	4.000	4.000	4.000	4.000	4.000	4.000
Al	1.291	1.302	1.553	1.268	1.401	1.500	1.217	1.256	1.272	1.217
Ti	0.006	0.004	0.005	0.006	0.005	0.005	0.016	0.008	0.005	0.016
Fe	1.543	1.460	2.185	2.233	2.173	2.213	1.572	2.353	2.327	1.572
Mn	0.022	0.019	0.025	0.010	0.025	0.026	0.004	0.006	0.015	0.004
Mg	3.072	3.140	1.662	2.326	2.192	2.232	2.979	2.275	2.350	2.979
Ca	0.008	–	0.032	0.009	0.016	0.016	0.025	0.013	0.022	0.025
Na	–	0.002	0.018	–	0.004	0.004	–	0.004	0.004	–
K	0.001	0.001	0.039	0.004	0.004	0.004	0.016	0.004	0.004	0.016
Fe/Fe+Mg	0.33	0.32	0.43	0.49	0.50	0.51	0.35	0.49	0.50	0.65
Cl_xChl_y)	52:26	53:25	30:40	40:38	38:38	37:37	51:27	39:40	39:39	52:27

variety: Fe-clinochlore /Al-Mg – chamosite / clinochlore / Al-Mg-chamosite/ Fe-clinochlore/
*All iron assumming as Fe^{2+}

Table 7
Ilmenites, selected analyses (wt %)

	Retrogaded eclogite	massive amphibolite	banded amphibolite	banded amphibolite
	KH-34, Poličany	KH-31 Víska	KH-6, Třebonín	KH-17, Malešov
SiO_2(%)	–	–	–	–
TiO_2	50.67	56.93	50.40	50.99
Al_2O_3	–	0.06	0.02	0.01
FeO	47.66	41.78	47.63	45.83
MnO	1.28	0.96	1.80	2.70
MgO	0.25	0.05	0.07	0.34
CaO	0.12	0.21	0.08	0.13
total	99.98	99.99	100.00	100.00
Si	–	–	–	–
Ti	1.916	2.169	1.908	1.926
Al	–	0.004	0.001	0.001
Fe^{3+}	0.168	–	0.184	0.146
Fe^{2+}	1.836	1.771	1.821	1.779
Mn	0.055	0.041	0.077	0.115
Mg	0.019	0.004	0.005	0.025
Ca	0.006	0.011	0.004	0.007
Fe^{2+}%	96.79	97.11	95.74	93.59
Mn %	2.87	2.26	4.03	6.04
Ca %	0.34	0.62	0.23	0.37

Appendix 4
P-T estimates

Table 1
Garnet-amphibole and amphibole-plagioclase geothermometers (Graham and Powell 1984, Blundy and Holland 1990), composition of minerals (wt %)

	Gt	Am	Gt	Am	Gt	Am	Gt	Am	Gt	Am	Gt	Am
	KH-25 (Libodřice)		KH-34 (Poličany)		KH-32 (Poličany)		KH-21 (Na skalce)		KH-23 (Na skalce)		KH-35 Žehušice	
	retrogr. eclogite		least retrograded eclogite				retrograded eclogite				gt. amphibolite	
SiO_2(%)	38.78	44.91	42.59	43.13	28.79	42.80	38.85	43.94	35.66	41.50	42.93	44.37
TiO_2	0.17	0.88	0.55	0.52	0.03	0.44	0.11	0.86	0.20	1.31	1.25	1.04
Al_2O_3	23.25	10.75	17.55	14.31	14.98	12.20	20.04	11.72	22.31	12.85	14.42	12.36
Cr_2O_3	0.07	0.04	n.d.	n.d.	n.d.	n.d.	n.d.	n.d.	0.00	0.00	0.00	0.00
FeO	24.52	17.62	16.81	15.71	18.93	10.74	25.40	17.72	25.55	14.99	15.78	13.77
MnO	0.24	0.11	0.20	0.24	0.25	0.29	1.56	0.09	0.84	0.04	0.26	0.29
MgO	3.66	10.67	10.65	11.06	19.56	14.70	1.70	9.76	1.48	11.31	11.29	11.62
CaO	9.24	9.94	11.64	8.36	17.40	13.89	12.29	10.84	13.90	12.54	14.04	13.45
Na_2O	-	1.98	-	3.47	-	1.47	-	2.05	-	2.39	-	1.29
K_2O	-	0.06	-	0.17	-	0.69	-	0.08	-	0.07	-	0.10
total	99.93	96.96	99.99	98.67	99.94	97.22	99.95	97.06	99.94	97.00	99.97	98.29
MgO/MgO + FeO	0.21	0.52	0.53	0.56	0.65	0.71	0.11	0.49	0.09	0.57	0.56	0.60
Si	6.005	6.728	6.403	6.419	4.670	6.322	6.152	6.606	5.697	6.242	6.499	6.502
Al	-	1.272	-	1.581	1.330	1.678	-	1.394	0.303	1.758	-	1.498
Al	4.243	0.625	3.111	0.929	1.534	0.445	3.740	0.682	3.897	0.520	2.573	0.636
Ti	0.020	0.099	0.026	0.058	0.004	0.049	0.013	0.097	0.024	0.148	0.142	0.115
Cr	0.003	0.005	-	-	-	-	-	-	-	-	-	-
Fe^{3+}	-	0.377	-	0.312	-	-	-	0.406	0.331	-	0.073	-
Mg	0.845	2.383	2.388	2.453	4.730	3.237	0.401	2.287	0.352	2.536	2.548	2.538
Fe^{2+}	-	1.511	-	1.247	1.538	1.269	-	1.627	3.082	1.796	1.925	1.687
Fe^{2+}	3.175	0.319	2.114	0.397	-	0.058	3.364	0.195	-	0.090	-	-
Mn	0.031	0.014	0.026	0.030	0.034	0.036	0.209	0.011	0.114	0.005	0.034	0.012
Ca	1.533	1.595	1.874	1.333	3.024	1.906	2.085	1.746	2.379	1.905	2.278	1.988
Na	-	0.071	-	0.240	-	-	-	0.048	-	-	-	-
Ca	-	-	-	-	-	0.292	-	-	-	0.116	-	0.124
Na	-	0.504	-	0.762	-	0.421	-	0.550	-	0.695	-	0.366
K	-	0.011	-	0.013	-	0.130	-	0.015	-	0.013	-	0.019
P^1(kbar)	Gt-Am	14.1		18.5		20.1		12.6		14.0		19.7
P^2(kbar)	Am-Pl	15.7		16.9		15.3		13.6		13.7		13.3
T^1(°C)	Gt-Am	513		694		1 008		507		677		1244
T^2(°C)	Am-Pl	629		580		602		592		652		606

Note: Fixed $Fe^{3+}/(Fe^{3+} + Fe^{2+})$ ratio of 0.20 calculated on basis of 23 oxygens

Table 2
Amphibole-plagioclase geothermometer (Plyusnina 1982)

	AM	Pl	Am	Pl	Am	Pl	Am	Pl	Am	Pl	Am	Pl
	KH-8, Chedrbí		KH-19, Kbílek		KH-15, Markovice		KH-6, Třeboním		KH-13, Okřesaneč		KH-29, Hodkov	
	banded amphibolite				striped amphibolite				banded amphibolite			
SiO_2(%)	39.24	59.59	40.10	62.32	43.17	59.93	45.45	59.08	40.52	61.69	44.66	61.48
TiO_2	1.54	0.01	1.06	0.09	0.86	-	0.67	0.01	1.40	0.04	1.01	-
Al_2O_3	12.34	12.98	13.17	12.77	23.48	24.08	13.19	24.57	11.14	22.53	11.71	23.09
FeO	16.94	-	10.31	0.10	18.69	0.19	14.41	0.08	22.26	0.16	14.42	0.17
MnO	0.26	0.08	0.23	0.02	0.31	-	0.26	-	0.26	-	0.34	-
MgO	9.01	-	14.05	-	9.31	0.02	11.51	-	7.53	-	11.50	0.01
CaO	14.32	7.30	14.53	8.40	11.34	6.65	11.18	7.30	11.34	5.80	11.59	5.70
Na_2O	1.89	6.70	2.34	8.13	1.49	8.02	1.97	6.70	1.80	9.26	2.07	7.24
K_2O	1.54	0.08	0.68	0.21	0.41	0.11	0.39	0.08	1.22	0.19	0.39	0.03
total	98.73	97.82	98.19	100.94	96.98	99.00	98.03	97.82	97.47	99.67	97.69	97.72
Si	7.112	10.739	6.979	11.067	6.558	10.799	6.520	10.739	6.315	11.046	6.597	11.110
Al	0.888	-	1.021	-	1.442	-	1.480	-	1.685	-	1.403	-
Al	1.748	5.264	1.681	4.535	0.590	5.114	0.801	5.264	0.361	4.754	0.636	4.918
Ti	0.210	0.001	0.139	0.012	0.098	-	0.074	0.001	0.164	0.005	0.112	-
Fe^{3+}	0.121	0.012	-	0.015	0.438	0.029	-	0.012	-	0.024	-	0.026
Mg	2.434	-	3.180	-	2.120	0.005	2.517	-	1.750	-	2.532	0.003
Fe^{2+}	0.487	-	-	-	1.754	-	1.608	-	2.725	-	1.720	-
Fe^{2+}	1.960	-	1.501	-	0.183	-	0.159	-	0.176	-	0.062	-
Mn	0.040	-	0.034	0.003	0.040	0.003	0.032	-	0.034	-	0.043	-
Ca	2.781	-	2.710	-	1.777	-	1.757	-	1.789	-	1.834	-
Na	-	-	-	-	-	-	0.051	-	-	-	0.062	-
Ca	-	1.422	-	1.598	0.068	1.284	-	1.422	0.104	1.113	-	1.104
Na	0.664	2.361	0.790	2.799	0.439	2.802	0.509	2.361	0.544	3.215	0.531	2.537
K	0.356	0.019	0.151	0.048	0.079	0.025	0.073	0.019	0.243	0.043	0.073	0.007
Al^{tot}Am	2.636		2.702		2.032		2.281		2.046		2.039	
An (mol.%)		37.4		36.0		31.2		37.4		25.4		30.2
P (kbar)	7.7		8.0		5.1		6.2		5.2		5.1	
T (°C)		550		555		542		575		530		540

Table 3
Amphibole-plagioclase geothermometer (Plyusnina 1982)

	Am	Pl	Am	Pl	Am	Pl	Am	Pl
	KH-17, Malešov		KH-3, Č. Šternberk		KH-22, Mančice		KH-31, Víska	
	banded amphibolite		massive amphibolite				massive amphibolite	
SiO_2(%)	45.25	62.36	45.25	58.79	48.38	67.09	44.60	63.69
TiO_2	0.45	–	1.00	–	0.59	–	0.66	0.01
Al_2O_3	11.51	24.19	11.18	26.14	8.95	19.87	12.68	22.89
FeO	14.15	0.08	16.93	0.25	11.90	0.07	13.92	0.15
MnO	0.22	–	0.32	0.04	0.13	0.04	0.26	–
MgO	11.96	0.02	9.05	0.01	14.24	0.02	13.20	–
CaO	11.93	6.38	11.54	7.28	10.74	2.91	10.49	4.73
Na_2O	1.49	6.88	1.76	7.43	1.97	9.96	2.69	8.51
K_2O	0.27	0.08	0.35	0.05	0.07	0.03	0.22	0.01
total	97.23	99.99	97.34	99.99	96.97	99.99	98.72	99.99
Si	6.681	11.016	6.759	10.505	7.033	11.782	6.487	11.240
Al	1.319	–	1.241	–	0.967	–	1.513	–
Al	0.684	5.037	0.727	5.505	0.566	4.112	0.660	4.761
Ti	0.050	–	0.112	–	0.064	–	0.072	0.001
Mg	2.633	0.005	2.015	0.003	3.086	0.005	2.862	–
Fe	1.633	0.012	2.115	0.037	1.283	0.010	1.405	0.022
Mn	–	–	0.031	0.006	–	0.006	–	–
Fe	0.114	–	–	–	0.163	–	0.288	–
Mn	028	–	0.010	–	0.016	–	0.032	–
Ca	1.859	–	1.847	–	1.673	–	1.635	–
Na	–	–	0.143	–	0.148	–	0.046	–
Ca	0.029	1.208	–	1.395	–	0.548	–	0.895
Na	0.427	2.357	0.366	2.574	0.407	3.967	0.713	2.914
K	0.051	0.018	0.067	0.011	0.013	0.007	0.041	0.002
$Al^{tot}Am$	2.003		1.968		1.533		2.173	
An (mol %)		33.7		35.0		13.9		23.5
P (kbar)	5.0		4.9		3.0		5.7	
T (°C)		556		562		507		544